1-1-2013

Effect Of Electrochemical Modification On The Surface Topography And Chemical Make-Up Of Strontium Titanate

Kelly J. Harmon
Eastern Illinois University

THESIS MAINTENANCE AND REPRODUCTION CERTIFICATE

TO: Graduate Degree Candidates (who have written formal theses)

SUBJECT: Permission to Reproduce Theses

An important part of Booth Library at Eastern Illinois University's ongoing mission is to preserve and provide access to works of scholarship. In order to further this goal, Booth Library makes all theses produced at Eastern Illinois University available for personal study, research, and other not-for-profit educational purposes. Under 17 U.S.C. § 108, the library may reproduce and distribute a copy without infringing on copyright; however, professional courtesy dictates that permission be requested from the author before doing so.

By signing this form:

- You confirm your authorship of the thesis.
- You retain the copyright and intellectual property rights associated with the original research, creative activity, and intellectual or artistic content of the thesis.
- You certify your compliance with federal copyright law (Title 17 of the U.S. Code) and your right to authorize reproduction and distribution of all copyrighted material included in your thesis.
- You grant Booth Library the non-exclusive, perpetual right to make copies of your thesis, freely and publicly available without restriction, by means of any current or successive technology, including but not limited to photocopying, microfilm, digitization, or Internet.
- You acknowledge that by depositing your thesis with Booth LIbrary, your work is available for viewing by the public and may be borrowed through the library's circulation and interlibrary departmenst or accessed electronically.
- You waive the confidentiality provisions of the Family Educational Rights and Privacy Act (FERPA) (20 U.S.C. § 1232g; 34 CFR Part 99) with respect to the contents of the thesis, including your name and status as a student at Eastern Illinois Univerity.

Petition to Delay:

I respectfully petition that Booth Library delay maintenance and reproduction of my thesis until the date specified and for the reasons below. I understand that my degree will not be conferred until the thesis is available for maintenance and reproduction.

Date:

Reasons:

Holly Harmon 8/14/13

Author's Signature Date

This form must be submitted in duplicate.

The Effect of Electrochemical Modification on the Surface Topography and Chemical Make-up of Strontium Titanate

(TITLE)

BY

Kelly J. Harmon

THESIS

SUBMITTED IN PARTIAL FULFILLMENT OF THE REQUIREMENTS
FOR THE DEGREE OF

Master of Science in Chemistry

IN THE GRADUATE SCHOOL, EASTERN ILLINOIS UNIVERSITY
CHARLESTON, ILLINOIS

2013
YEAR

I HEREBY RECOMMEND THAT THIS THESIS BE ACCEPTED AS FULFILLING
THIS PART OF THE GRADUATE DEGREE CITED ABOVE

		Mark E McGuire	8-13-13
THESIS COMMITTEE CHAIR	DATE	DEPARTMENT/SCHOOL CHAIR OR CHAIR'S DESIGNEE	DATE
[signature]	7/16/13	[signature]	7/16/13
THESIS COMMITTEE MEMBER	DATE	THESIS COMMITTEE MEMBER	DATE
[signature]	7/16/13		
THESIS COMMITTEE MEMBER	DATE	THESIS COMMITTEE MEMBER	DATE

By: Kelly J. Harmon

Abstract

Previous research into the oxidation and reduction of strontium titanate and the changes that result from this has been carried out. The oxidation and reduction of strontium titanate at high temperatures and high pressures has been investigated for the effect that it has upon the surface topography of strontium titanate and the chemical makeup of the strontium titanate. Research into the electrochemical oxidation of perovskites, similar in structure to that of strontium titanate, have even provided evidence pointing to the identity of the oxygen species being incorporated into the strontium titanate.

This research seeks to investigate what changes occur to both the surface topography of strontium titanate and its chemical makeup upon electrochemical modification using atomic force microscopy and XPS spectroscopy respectively. The effects of varying the potential applied to the sample and the time that the sample was exposed to the potential were also investigated by exposing samples of strontium titanate to various potentials for various lengths of time.

The end result of this electrochemical modification was the observation that an exposure to a positive potential, and only a positive potential, causes triangular crystals of titanium dioxide to appear upon the surface of the strontium titanate where the sample was clipped to serve as the working electrode. It was also found that larger potentials being applied for greater lengths of time increases crystal size, number, and packing density. These triangular crystals were identified as being rutile titanium dioxide by X-ray diffraction testing. XPS spectroscopy reveled that some change was occurring with the oxygen present in the samples.

Acknowledgments

Dr. Svetlana Mitrovski

Dr. Mauro Sardela

Dr. Gopal Periyannan

Dr. Rick Haasch

This research was funded by the National Science Foundation, grant CHE-1039894.

Table of Contents

Table of Figures

The Effect of Electrochemical Modification on the Surface Topography and Chemical Make-up of Strontium Titanate

Introduction

Strontium titanate ($SrTiO_3$) is a compound that is arranged as a cubic perovskite under all but certain conditions.[1] This material has been used for a variety of purposes ranging from jewelry[2] to an oxygen detector. This ability of strontium titanate to absorb oxygen into its crystal structure forms the basis for the research outlined in this thesis. Various methods have been used in the past to oxidize strontium titanate or related materials; however, these methods have either required high temperatures[3] or did not focus upon changes in surface topology, instead focusing upon the changes in chemical makeup of the crystals and the electrochemistry occurring with the electrolyte.[4] The goal of this research is to oxidize and reduce samples of strontium titanate at room temperature and to investigate what effect this modification has upon the surface topology of the strontium titanate as well as the chemical makeup of the strontium titanate.

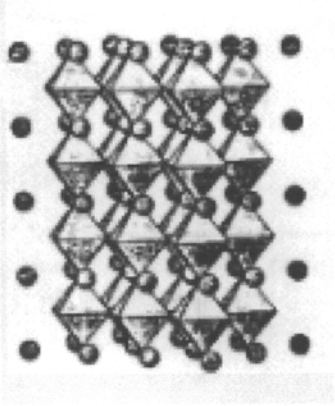

Figure 1: Crystal structure of strontium titanate. Octahedrons are titanium liganded to oxygens; spheres are strontium (Figure from reference 4)

Incorporation of Oxygen into Strontium Titanate

The mechanism for the incorporation of oxygen into strontium titanate from the gas phase at high temperature and pressure is known. This incorporation can be broken down into three major steps: incorporation at the surface, diffusion into the matrix of the strontium titanate, and diffusion along grain boundaries. When the oxygen is first incorporated into the surface of the strontium titanate it adsorbs onto the surface where the molecular oxygen is converted into O_2^-. This oxygen species is then converted into O_2^{2-} by electron transfer. After this is complete, the O_2^{2-} is further broken down into two O^- species.[5] That the O_2^{2-} forms during the adsorption of oxygen into other materials has been detected by high energy electron energy loss spectroscopy.[6] The oxygen anions are then incorporated into oxygen vacancies that exist within the structure of the strontium titanate.[5]

Once the oxygen has been incorporated into the vacancies in the surface layer of

the strontium titanate, it can begin to diffuse into the main body of the strontium titanate. The incorporated oxygen will then continue moving into the strontium titanate until such time as it reaches a grain boundary. The grain boundary serves as a barrier across which the transportation of the oxygen becomes much more difficult. This was demonstrated by the effect that the grain boundary had on measuring the concentration of oxygen present. When the measurements approach the grain boundary, the oxygen concentration increases suddenly as the boundary serves to impede the movement of the oxygen species. Thus, the oxygen will rapidly move along the grain boundaries due to this being easier than trying to move across the boundary.[5]

The incorporation of oxygen into related materials from a solution containing hydroxide ions using an electrochemical reaction works by breaking down the hydroxide ions in order to obtain the oxygen species that is to be incorporated into the structure of the cubic perovskite. Various samples of oxides containing strontium and other metals were exposed to positive potentials while placed in 1 M solution of either KOH or NaOH. The cyclic voltammogram produced from the use of a perovskite as the working electrode can be seen in Figure 2. As can be seen in this figure, the oxidation does not begin to occur until a potential of around 600 mV is applied to the oxide sample.[4]

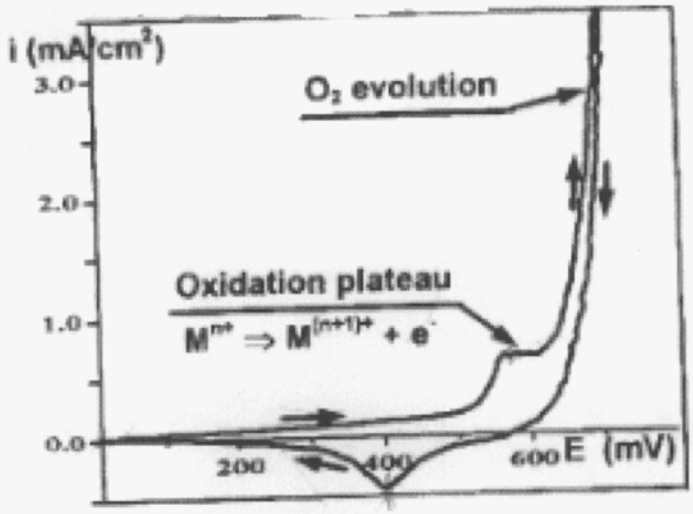

Figure 2: Cyclic voltammogram of a perovskite electrode in 1 M NaOH solution. Oxidation plateau and point that oxygen begins to be released from the hydroxide can be seen occurring at around 600 mV potential. (Figure from reference 4)

It is believed that the oxygen species incorporated into the material's structure is O^- anions. It is known that the oxidized materials do not contain hydroxide species (as was determined by NMR and IR spectroscopy), and the diffusion rate of the oxygen species does not match up with what would be expected of the larger O^{2-} species.[4]

Non-stochiometry of Perovskites

The filling of the previously mentioned oxygen vacancies in strontium titanate can have an effect upon the properties of strontium titanate. It is known that increasing the amount of oxygen present in strontium titanate can result in the electrical conductivity of the strontium titanate decreasing. Strontium titanate is not the only perovskite for which changes in the oxygen content can cause changes in the material's properties. $YBa_2Cu_3O_{6+\delta}$ is a cubic perovskite for which varying the stoichiometry of the oxygen can determine whether or not the material is a superconducter.[5] Other perovskites can be altered by doping them with other elements. The perovskite $LaFeO_3$, when doped with calcium, can be used as the catalyst in the catalytic combustion of methane.[7] Another

perovskite that has been doped with aluminum, $(Ba_{0.5}Sr_{0.5})$-$(Fe_{1-x}Al_x)O_{3-\delta}$, becomes increasingly permeable to oxygen with increased stochiometry of aluminum.[8] One other perovskite, $YBa_2Cu_3O_{7-\delta}$, which is a superconductor, has its superconductivity quenched by being doped with zinc.[9]

Oxidation and Reduction of Strontium Titanate at High Temperatures

Both the oxidation and the reduction of strontium titanate have been carried out at high temperatures in previous experiments. Under oxidizing conditions, it was found that temperatures in excess of 900 °C cause the formation of ridge like structures on the surface of crystals of strontium titanate, as can be seen in Figure 3.[3]

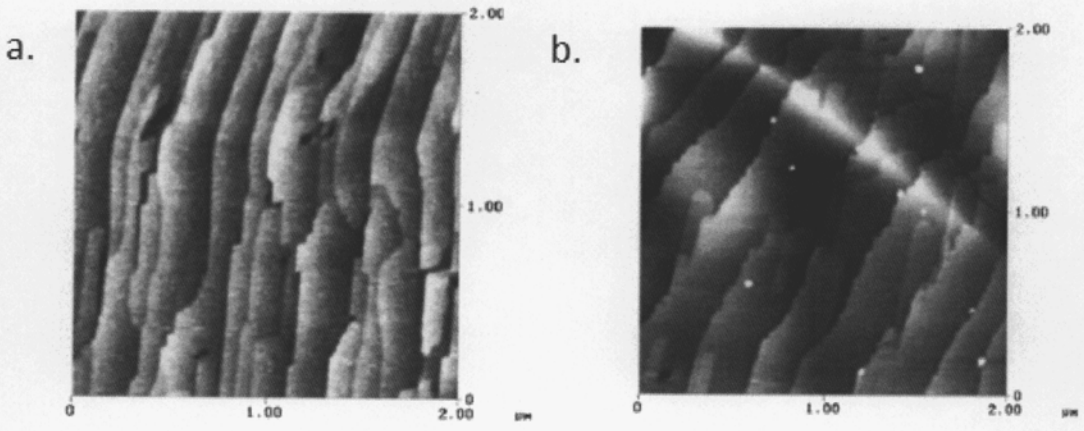

Figure 3: a.) Strontium titanate heated to 900 °C under oxidizing conditions. b.) Strontium titanate heated to 1000 °C under oxidizing conditions. (Figure from reference 3)

These ridge like structures were measured to have heights of approximately 11.8 Å and were found to be caused by the formation of a Ruddlesden-Popper (Sr_2TiO_4) phase upon the surface of the crystals. As can be seen in Figure 3, the higher temperature results

in more well defined ridges when the sample is being oxidized. Heating a sample of strontium titanate to similarly high temperatures under reducing conditions also results in changes to the surface topography of the strontium titanate crystal; in this case the formation of much less well defined ridges, as can be seen in Figure 4.[9]

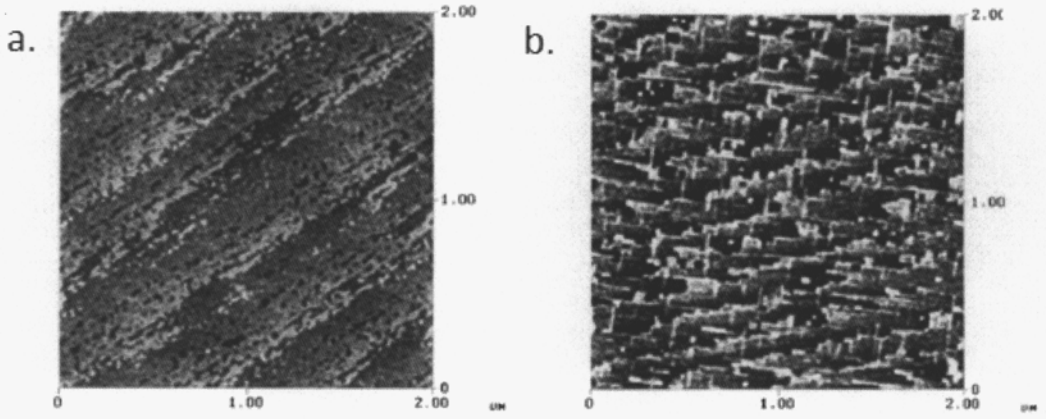

Figure 4: a.) Strontium titanate after being heated to 900 °C under reducing conditions. b.) Strontium titanate after being heated to 1000 °C under reducing conditions. (Figure from reference 3)

These ridges are caused by the formation of TiO and Ti_2O phases upon the surface of the crystal. As can be seen in this figure, the ridges become less well defined as the sample is heated from 900 °C to 1000 °C, unlike when the sample is oxidized. At the higher temperature, these ridges begin to become more random in how they are positioned on the strontium titanate sample.[3]

Observing the Changes

In order to actually observe the changes that took place upon the electrochemically modified strontium titanate, three different methods were used. The first was atomic force microscopy, which was used to observe changes in the surface

topography of the strontium titanate. In order to observe the crystal structure of the samples, X-ray diffractometry was used, and in order to observe changes to the chemical composition of the samples, X-ray photoelectron spectroscopy was used.

Atomic Force Microscopy

Atomic force microscopy (AFM) is an analytical method that allows for the nanoscale imaging of the surface topography of objects. This method has seen a variety of uses, ranging from investigating the organization of lipid bilayers[10] to imaging the surface topography of lymphoma cells[11] to investigating the electrodegradation of iron doped strontium titanate.[12] Atomic force microscopy represents an improvement over the earlier scanning tunneling microscopy. The later method can only really be used on materials that conduct electricity; however, atomic force microscopy can be used on a variety of materials, including ones that are insulating.[13]

In general, an atomic force microscope works by moving a tip attached to a cantilever along the surface of the material that is being studied. The tip of the atomic force microscopy probe can interact with the atoms that make up the surface of the material being studied as can be seen in Figure 5. While the tip is moved along the surface of the sample, it is held so that there is a constant force between it and the sample surface. These interactions cause deflection in the cantilever, which can be detected, related to the surface topography of the sample, and used to produce the AFM micrographs.[14]

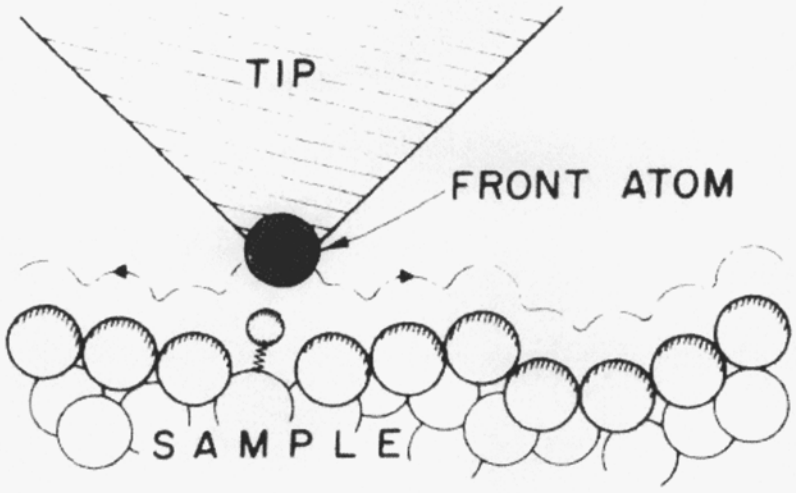

Figure 5: Illustration of the tip used in AFM. Atom at the end of tip interacts with the atoms of the sample, causing the tip to follow the surface topography of the sample when it is dragged along the sample's surface. (Figure from reference 14)

The forces that are involved in the interactions between the tip and the sample include both attractive and repulsive forces. These forces include but are not limited to Pauli repulsion forces, electrostatic forces, van der Waals forces, and dispersion forces. A graph showing how the forces acting upon the tip vary with regards to how close the tip is to the surface can be seen in Figure 6. As the gap between the tip and the surface of the sample is varied, the forces between the tip and the surface vary in whether attractive forces or repulsive forces dominate. As the tip approaches the sample, attractive forces dominate; however, when the tip reaches the right distance away from the sample, repulsive forces dominate. Continued use of a tip can alter the forces that are operating on the tip. As the tip is used, some debris can build up on the tip; this can cause increasing the tip to develop dipoles or even become charged, which will affect how the tip interacts with the materials being analyzed.[15]

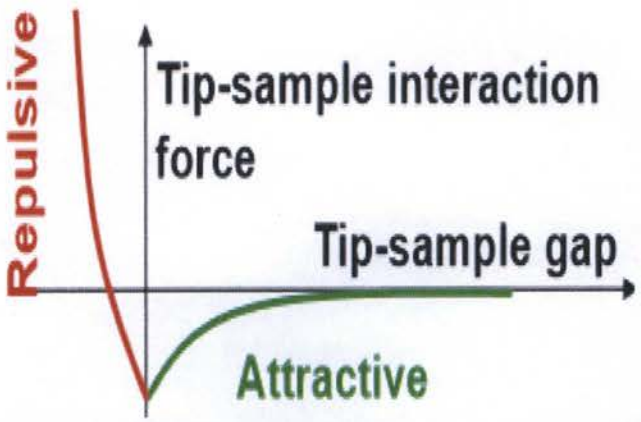

Figure 6: Diagram showing how force between tip and sample varies with regards to the gap between the sample and the tip. (Figure from reference 15)

Atomic force microscopy can be used in a variety of different modes; the two that are most important to the subject at hand are contact mode and semicontact mode. In contact mode, the tip is brought close enough to the sample that the thin layers of water (adsorbed from the atmospheric humidity) that forms on the tip and the sample cause the tip to be held in contact with the sample due to capillary forces. The tip is then moved along the sample where changes in the surface topography of the sample cause the tip to move with these changes due to repulsive force between the tip and the sample surface, and thus the cantilever begins to have changes in its deflection. This works similar to the general idea of how atomic force microscopy works as was explained above.[16]

For semicontact mode, the cantilever is oscillating at its natural frequency when it is brought near the sample surface, as is illustrated by Figure 7.[17] This causes the tip to only come into contact with the surface some of the time so that the tip taps the surface as it is moved along the surface. The cantilever still shows changes in its deflection as it interacts with the surface of the sample; in this case the changes manifest in the form of changes to the oscillation of the tip. This method does have certain advantages over the

contact method; the first of which is that this method is more sensitive to how it interacts with the surface of the sample. The other major advantage this method has is that it works better on samples that are more easily damaged due to the tip only coming into contact with the surface periodically.[16]

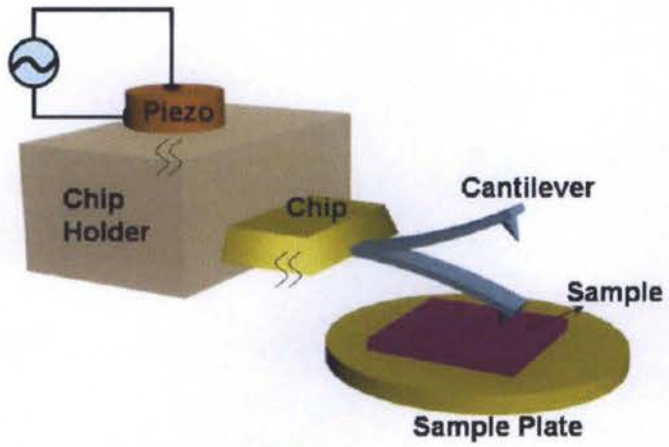

Figure 7: Illustration of oscillating cantilever. In semicontact mode, the cantilever is oscillated up and down so that the tip only periodically comes into contact with the sample. (Figure from reference 17).

The actual changes in the deflection of the cantilever have been detected in a variety of ways throughout the history of atomic force microscopy. When atomic force microscopy was first developed, the deflection of the cantilever was monitored by placing a scanning tunneling microscope on the back of the cantilever as can be seen in Figure 8.[14] The method (modeled in Figure 9) that is most commonly used today involves shining a laser onto the cantilever; the beam from the laser is reflected off of the cantilever to where it is detected by a photodiode. Any changes in the deflection of the cantilever will cause where the reflected laser beam is on the photodiode to change, thus allowing the deflection of the cantilever to be monitored by noting changes that occur in the voltage produced by the photodiode. The AFM is able to maintain a constant force

upon the sample by moving the sample itself up or down as is necessary (see Figure 10).[13]

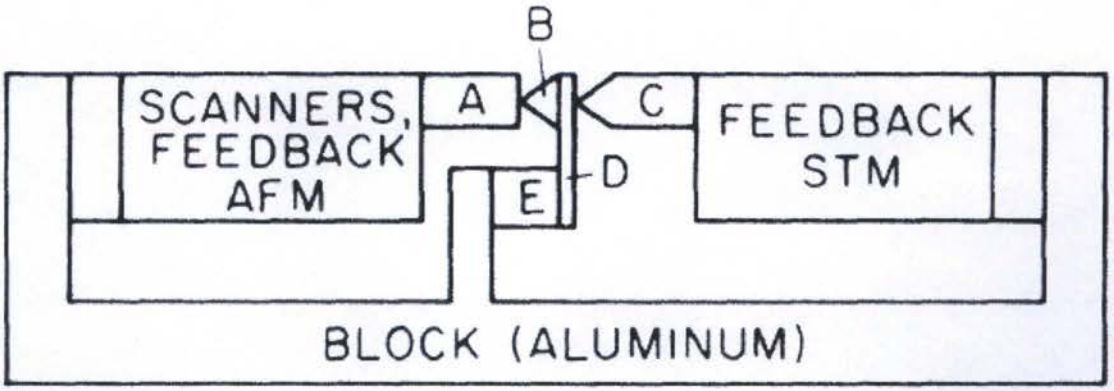

Figure 8: Illustration of first form of atomic force microscopy. A is the sample, B is the AFM tip, C is the scanning tunneling microscope tip, D is the cantilever, and E is the modulating piezo. The scanning tunneling microscope placed on the back of the cantilever detects deflections in the cantilever caused by interactions between AFM tip and the sample surface. (Figure from reference 14)

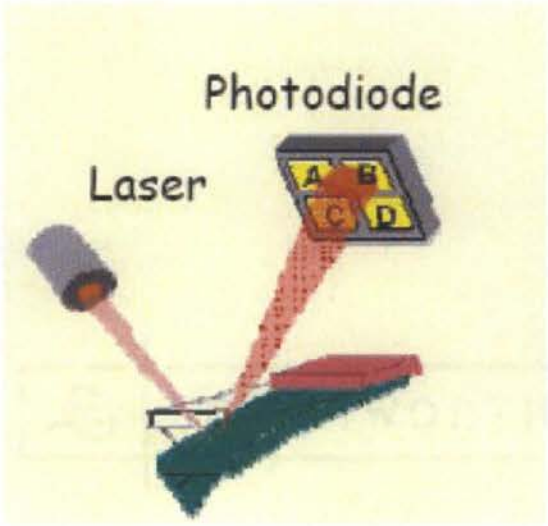

Figure 9: Illustration of modern method of detecting cantilever deflection. Laser is shone upon the cantilever, which reflects the laser upon a photodiode. Any movement of the cantilever, such as is caused by the tip moving due to its interaction with the sample surface, changes where the reflected laser shines upon the photodiode. This would cause changes in voltage produced by the photodiode. (Figure from reference 13)

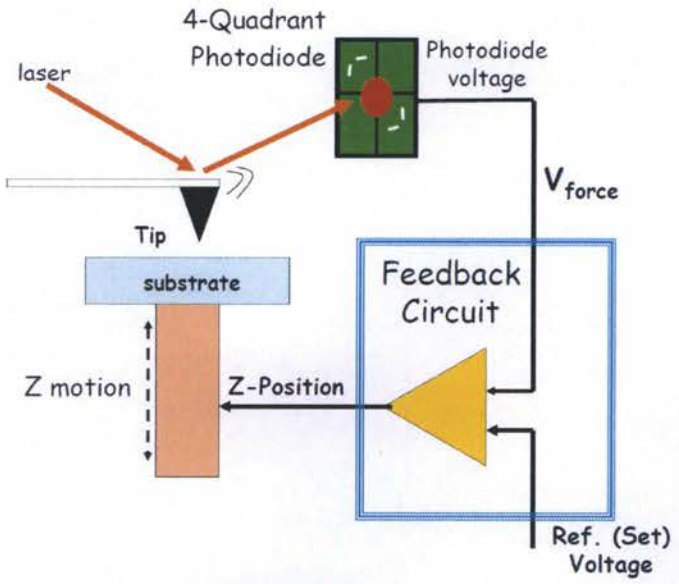

Figure 10: Illustration of how AFM keeps a constant force in modern AFM. Information from the photodiode is fed into feedback circuit, which is used to determine position of substrate. Substrate moves up or down with sample as is needed to maintain constant force. (Figure from reference 13)

X-Ray Diffractometry

X-ray diffractometry is another method that was used to characterize the modified samples produced during the course of this research. In particular, X-ray diffractometry can be used to identify the compounds present in the sample by matching the X-ray diffraction pattern with those of known crystals. An example of how an X-ray diffractometer is generally set up can be seen in Figure 11. In X-ray diffractometry, the sample is bombarded with X-rays; the X-ray photons are scattered when they collide with the electrons of the sample's atoms. This is able to work because the wavelengths of the x-rays are close in magnitude to the length of space between the atoms of the samples. The pattern formed from this scattering can be used to identify the crystals present on the sample. This method can be used to probe below the surface of the sample.[18]

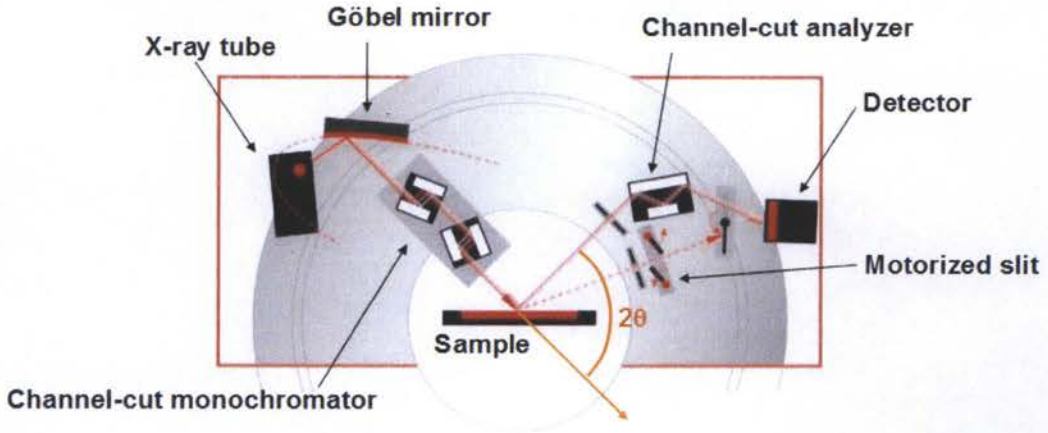

Figure 11: Typical set-up used for x-ray diffractometry. Sample is bombarded with X-rays produced in X-ray tube, which deflect off of electrons in sample. The Göbel mirror and channel cut monochromator are used to direct the X-rays of the desired wavelengths towards the sample. These deflected X-ray photons are picked up by the detector. (Figure from reference 18)

X-Ray Photoelectron Spectroscopy

The final method that was used during the course of this research to analyze the results was X-ray photoelectron spectroscopy (XPS). Like with X-ray diffractometry, the sample is bombarded with X-rays; however, unlike X-ray diffractometry, XPS uses the X-ray photons to remove electrons from the sample, as demonstrated in Figure 12. Since the electron structures of the various different elements are unique, the kinetic energies of the electrons emitted from the atoms will be unique to the element as well. Since the energy of the X-ray photons is known and the kinetic energies of the electrons are measured, the binding energy of the electrons can be calculated by measuring the difference between the two. The information generated from this can be used to calculate the percentage of each element present in the sample, as well as providing information about the chemical environment of the elements present in the sample. Unlike X-ray

diffractometry, XPS is used to analyze the surface of the sample.[19]

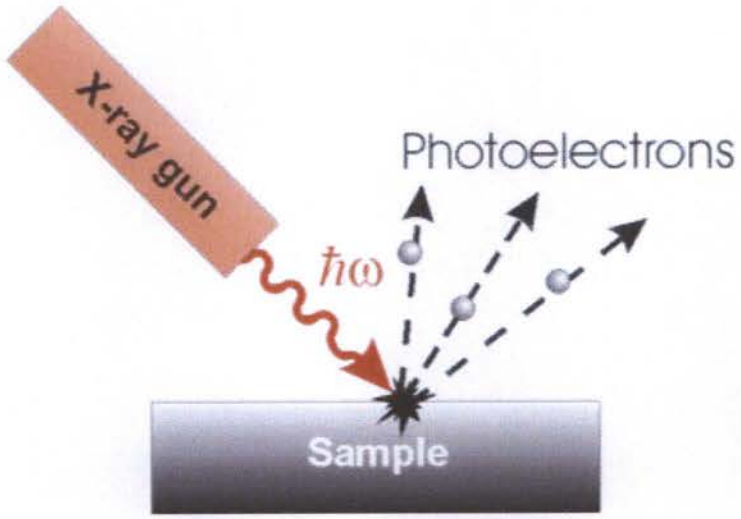

Figure 12: Illustration of how X-ray photons are used to expel electrons from the surface of a sample, as is done in XPS. (Figure from reference 19)

XPS of Strontium Titanate

XPS spectra have been collected from samples of strontium titanate that have been annealed at high temperatures. These spectra allow for the detection of the elements that are present in the sample of strontium titanate: strontium, titanium, oxygen, and even some carbon present on the surface of the sample. As can be seen in Figure 13, both the Sr 3d and the Ti 2p produce two peaks that can be seen in their XPS spectra. The XPS spectra for C 1s have one peak for itself, but there is a single peak for one of the spectra caused by Sr $3p_{1/2}$ present near the peaks for C 1s which is absent at 25 °C. The most interesting spectra out of all of these are those for O 1s; these spectra have an unusual shoulder that appears off of the main peak. This shoulder is more pronounced for the

strontium titanate at 25 °C practically disappearing at 800 °C.[20]It is likely that both the effect noted for the C 1s spectra and the O 1 s spectra are due to the heating eliminating carbonate contamination.

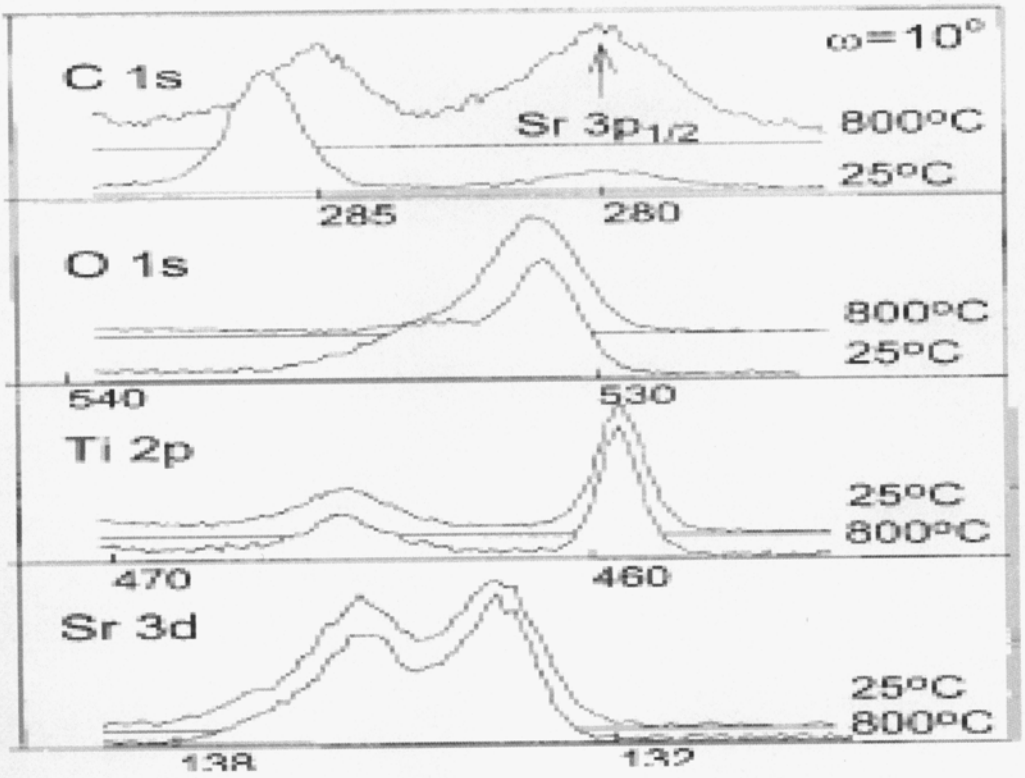

Figure 13: XPS spectra for annealed strontium titanate at both 25 °C and 800 °C. (Figure from reference 20)

Introduction Summary

Previous work has been done on the oxidation and reduction of strontium titanate or other similar compounds. However, most of the work that has been done on oxidizing or reducing strontium titanate has required heating the samples to high temperatures. These samples of strontium titanate that were oxidized and reduced at high temperatures were investigated for both changes in chemical composition and changes in surface topography. There were some instances of oxidizing compounds that were closely related to strontium titanate at room temperature using electrochemistry; however, these efforts

have focused more upon understanding how the oxygen is incorporated into the compound in question. This thesis will seek to investigate the effects of electrochemical oxidation and reduction upon the surface topography and the chemical makeup of samples of strontium titanate.

Materials and Methods

Materials

The strontium titanate (100) samples used in this research were purchased from MTI Corporation (Richmond, California, USA). The electrolyte that was used in the electrochemical cell was a 1 M NaOH solution prepared by dissolving 99.99% sodium hydroxide purchased from Sigma-Aldrich Corporation (St. Louis, Missouri, USA) in10 MΩ Millipore water.

Instrumentation

Electrochemistry

The samples of strontium titanate were used as the working electrodes for a CHI 660C potentiostat/galvanostat purchased from CHI Instruments (Austin, Texas, USA). In order to serve as the working electrode, the strontium titanate samples were clipped with a gold-coated alligator clip purchased from Pomona Electronics (Everett, Washington, USA). The counter electrode in this case is a platinum wire, and the reference electrode is a Hg/HgO electrode purchased from CHI Instruments (Austin, Texas, USA).

Atomic Force Microscopy

The AFM that was used to identify changes in the surface topography of the strontium titanate samples was an Ntegra Prima scanning probe microscope purchased from SPM; NT-MDT (Zelenograd, Russia). The tips that were used in this research were a mixture of Tap300Al-G tips (resonant frequency of approximately 300 kHz and force constant of 40 N/m) purchased from Budget Sensors (Sofia, Bulgaria) and NSG 10 tips (resonant frequency of approximately 240 kHz and force constant of 11.8 N/m) purchased from SPM; NT-MDT (Zelenograd, Russia).

X-Ray Diffraction

The x-ray diffractometer used to identify the chemical changes taking place was a PANalytical / Philips X'pert MRD system # 1 manufactured by PANalytical Inc. (Almelo, The Netherlands).

X-Ray Photoelectron Spectroscopy

The x-ray photoelectron spectroscopy was performed using a Kratos Axis XPS spectrometer manufactured by Kratos Analytical Ltd. (Manchester, United Kingdom).

Methods

Sample Preparation

In order to clean the samples prior to electrochemical modification, the samples were sonicated in acetone for five minutes followed by being sonicated in isopropyl alcohol for a similar length of time. Those samples of strontium titanate that proved to be rather large were broken up using a diamond edge cutter.

Electrochemical Modification

The electrochemical cell was set up in a manner similar to Figure 14. Within this electrochemical cell, the samples of strontium titanate were exposed to various positive and negative potentials for various lengths of time.

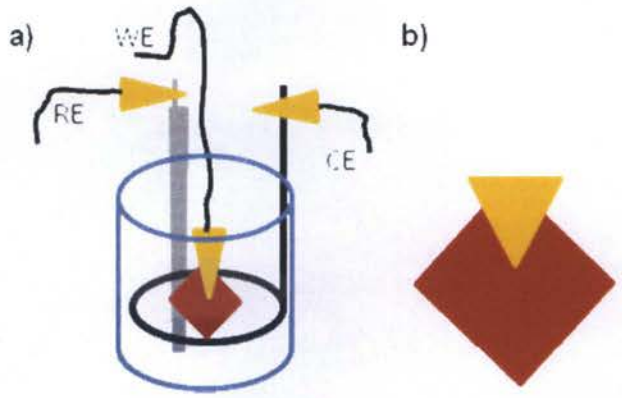

Figure 14: Illustration of the set-up used to electrochemically modify the strontium titanate. a.) The overall set-up, showing strontium titanate as the working electrode (WE), the Hg/HgO electrode as the reference electrode (RE), and the platinum wire as the counter electrode (CE). b.) Illustration of how the strontium titanate was clipped using the gold alligator clip.

Atomic Force Microscopy

The surface topography of the electrochemically modified samples of strontium titanate was investigated using atomic force microscopy in semicontact mode. The FB (feedback) gain, set point, preamplifier gain, preamplifier amplitude, and frequency of scan were set in order to obtain the results where the surface topography could be clearly seen.

X-Ray Diffraction

All measurements were made using thin-film optics with monochromator, and point-focus Cu radiation with wavelength of $\lambda_{Cu} = 0.15418$ nm.

X-Ray Photoelectron Spectroscopy

Survey XPS measurements were performed using Kratos Axis ultra-spectrometer using Al Kα monochromatic radiation of (12 kV, 180 W). Photoelectrons were analyzed using a hemispherical analyzer with constant pass energy of 160 eV for survey (low resolution) spectra. High resolution core level spectra corresponding to O1s, Ti2p, Sr3d

and C1s were taken using the same radiation (8 kV, 120 W). Photoelectrons were analyzed using constant pass energy of 20 eV.

Data Analysis

Electrochemical Modification

The charge values for the various electrochemical modifications were calculated by integrating the amperometric i-t curves using the software that came with the potentiostat.

Atomic Force Microscopy

The AFM micrographs of the strontium titanate were processed using NOVA SPM software. All of the micrographs were subjected to having a third order surface background removed in order to flatten out the sample and get clearer image. The scales of the micrographs were adjusted as was necessary to be able to see the all of the details present. In addition to this, the images were filtered to remove low frequency noise, when doing so would produce a sharper image. In order to measure the size ranges of the crystals, a minimum of ten crystals was needed to establish an effective measurement. The lengths were determined by measuring the crystals along their longest edges, and the heights were determined by measuring the crystals in order to find their highest points. The average roughness was determined by measuring the average roughness of several different areas of the same size on the samples using the analysis software that comes with the AFM and averaging these values together. Average roughness is calculated using equation 1.[21] Average roughness measures deviations in height from an average height of the sample.

$$R_a = \frac{1}{MN}\sum_{i=1}^{M}\sum_{j=1}^{N}\left|Zji\right|$$

Equation 1: Equation for calculating average roughness. M and N are the number of data points taken in both the x and y directions, and Z is the height of the surface relative to an average plane. (Equation from Reference 21)

Results

Electrochemistry of Strontium Titanate and Observed Problems

During the course of electrochemically modifying the samples of strontium titanate, it was found that an exposure to a positive potential resulted in the area where the strontium titanate was clipped darkening, often to an almost black color, as can be seen in Figure 15. Cyclic voltammograms were obtained using strontium titanate as the working electrode in order to compare them to that seen in Figure 2. In Figure 16, the cyclic voltammogram taken for potentials ranging from 0 V to 0.8 V can be seen. The oxidation plateau that was seen in the cyclic voltammogram in Figure 2 can also be clearly seen in this cyclic voltammogram. In comparing these two cyclic voltammograms, the largest differences that can be seen are that the current associated with the oxidation plateau for this sample of strontium titanate is approximately four times higher than that for the perovskite sample used in earlier research and that the area associated with oxygen evolution is only starting in the cyclic voltammogram of strontium titanate. The cyclic voltammogram taken for potentials ranging from 0 V to 1.0 V seen in Figure 17 is even closer in appearance to that produced by earlier research. The oxidation plateau comes in at a similar current, and the section associated with oxygen evolution is well developed in this cyclic voltammogram. The same can be said for the cyclic voltammogram taken from potentials ranging from 0 V to 1.2 V that can be seen in Figure 18; it too is similar in design to the cyclic voltammogram of the perovskite seen in Figure 2. This is fairly good evidence that the reaction taking place is indeed the oxygen incorporation noted in previous research.

However, the electrochemical modification of strontium titanate was not without

problems. One of the first problems to be encountered was the evaporation of the electrolyte. It was found that the sodium hydroxide could evaporate to such a degree that the strontium titanate could be left outside of the sodium hydroxide. The effects of this can be seen in Figure 19, an amperometric i-t curve for an electrochemical modification of strontium titanate that was left to be modified overnight. At some point during the electrochemical modification, the sample left the sodium hydroxide which caused the current being applied to the strontium hydroxide to drop down to close to zero. It was only when this was discovered the next morning and the sample was placed back under the surface of the sodium hydroxide that the current was able to go back up to levels similar to where it was prior to the evaporation occurring. This would seem to only be a problem for samples of strontium titanate that are exposed to an electrical current for long enough periods of time for the sodium hydroxide to experience significant evaporation. This problem could be avoided by using a sufficiently large sample of strontium titante; that way even if evaporation occurs, there will still be a sufficiently large enough amount of strontium titante still submerged to continue the electrochemical modification.

The other major problem that occurred seemed to be caused by the equipment used to electrochemically modify the sample of strontium titanate. During the course of the research, it was noticed that the current flow was beginning to decrease to far smaller numbers than what would be needed to produce the darkening of the clipped end, which was of interest to study; in this case currents on the order of 10^{-3} amps are where the darkening of the clipped end began. The first step that was taken in order to remedy this was moving the reference electrode closer to the working electrode. The results of this, seen in the cyclic voltammogram of Figure 20 and the amperometric i-t curve of Figure

21, were not promising. The current produced was still far too low to darken the clipped end. In an effort to get better results, a new set-up was devised, in which the positions of the working electrode and the reference electrode were held at fixed points through the use of three-pronged clamps. A cyclic voltammogram, Figure 22, produced using this set-up showed that the current was once again back up to the level needed to electrochemically modify a sample of strontium titanate. The amperometric i-t curves produced at 1.0 V and 1.2 V, Figures 23 and 24 respectively, give further evidence of this set-up allowing for a stronger current.

This improvement did not last long; as seen in the cyclic voltammogram of Figure 25, the currents again decreased to an unusable level, even with the improved set-up. This time a small negative current was produced, even with a positive potential being applied. Examination of the electrode leads of the potentiostat showed evidence of significant corrosion. Seeing as this was the most likely suspect for the decrease in current, new leads were obtained. Using these new leads gave a significant improvement, as can be seen in the amperometric i-t curve of Figure 26. The current once again reaches an acceptable level for the electrochemical modification of strontium titanate. This brings up a major concern with the electrochemical modification of strontium titanate: the electrode leads may often be near sodium hydroxide which can corrode the leads; in order to avoid this, care must be taken to minimize the contact that the sodium hydroxide has with the electrode leads or if possible obtain gold plated leads that will be resistant to corrosion. However, with normal electrode leads, corrosion may still occur; therefore, the electrode leads should be periodically checked for evidence of corrosion.

Changes to Surface Topography

In order to understand what happened during the electrochemical modification, it is necessary to study what changes both a positive and negative potential had upon the surface topography of the sample of strontium titanate. As can be seen in Figure 27, a positive potential, and only a positive potential, results in the formation of triangular crystals (later identified as rutile titanium dioxide) upon the surface of the strontium titanate. The sample exposed to a negative potential has no major difference between it and the unmodified sample of strontium titanate in terms of surface topography.

These crystals of titanium dioxide were found to only form upon the area where the strontium titanate was clipped. As can be seen in Figure 28, the number of triangular crystals drops off sharply once you get away from the blackened area where the sample was clipped. The areas outside of where the strontium titanate was clipped are much flatter and have fewer and smaller features in terms of surface topography.

Now that it has been established that positive potentials can cause the formation of these triangular crystals, it becomes necessary to see how varying the potential and the time exposed to the potential can change the surface topography. As seen in Figure 29, when the time exposed to the potential is kept at a constant 20 hours and the potential is varied, a higher potential results in the formation of larger more densely packed crystals. When the strontium titanate was exposed to 0.8 V for 20 hours, the crystals that did form were arranged in small clumps. The surface of the sample was not densely packed; there were large areas of relatively flat space all along the surface of the sample. These crystals are also relatively small, with heights ranging from 0.9 μm-1.1 μm and lengths ranging from 1.7 μm-2.0 μm. The crystals formed by exposing the strontium titanate to 1.0 V for

20 hours are larger and much more densely packed, with fewer and smaller flattened areas. Measurements of the crystal sizes for this sample placed them as having heights ranging from 2.8 μm-3.5 μm and lengths ranging from 4.9 μm-6.5 μm. Exposing the sample to 1.2 V for 20 hours showed an even greater increase in crystal density. The crystals are so densely packed in parts that there are no flattened areas present, and as such, it is not possible to get an accurate measure of the crystals heights. Measurements of the lengths place these crystals as ranging from 2.4 μm-6.0 μm.

Turning from an examination of the effects of varying the potential to varying the time exposed to the potential, it can be seen in Figure 30 that there is a general trend towards larger more densely packed crystals as the length of time increases. However, there are some exceptions to this general trend. A variety of samples were exposed to a potential of 0.8 V for various lengths of time. The shortest length of time for exposure was two hours. This resulted in the formation of a small number of crystals with lengths ranging from 2.3 μm-3.0 μm and heights ranging from 0.6 μm-1.2 μm. Exposing a sample of strontium titanate to the same potential for four hours resulted in the formation a large number of small crystals that have lengths of approximately 1.0 μm and heights ranging from 300 nm-350 nm. An exposure to the 0.8 V potential for six hours caused a few clumps of the triangular crystals to form on the surface of the strontium titanate sample. These crystals were measured to have lengths ranging from 0.5 μm-1.0 μm and heights ranging from 16 nm-23 nm. The effects of an exposure to 0.8 V for 20 hours have been previously mentioned.

These exceptions to the general trend raise the question of whether or not there is a better indicator of how the surface topography will end up being changed. An obvious

choice would be the total charge that was run through the sample. The charge is affected by both the potential and the time exposed to the potential. Also, comparisons of charge and changes to surface topography allow for comparisons between samples of different sizes. Larger samples are capable of having a greater surface area submerged in the sodium hydroxide than smaller samples; a larger surface area being submerged can result in a larger current flowing through the sample and thus a larger charge being applied to the sample. As seen in Figure 31 and Figure 32, it would seem that a larger charge generally results in larger more numerous crystals being formed on the surface of the strontium titanate.

The application of 0.689 C of charge resulted in the formation of a large number of small crystals with lengths of approximately 1.0 μm and heights ranging from 300 nm-350 nm. Another sample of strontium titanate had a charge of 1.25 C applied to it; this resulted in the formation of a small number of slightly larger crystals, with lengths ranging from 2.3 μm-3.0 μm heights ranging from 0.6 μm-1.2 μm. Applying a charge of 5.4 C to another strontium titanate sample resulted in the formation of a small number of small crystals with lengths measured to range from 0.5 μm-1.0 μm and heights measured to range from 16 nm-23 nm. The application of 10.75 C of charge resulted in the formation of a large number of small crystals with heights of approximately 200 nm and lengths ranging from 0.6 μm-1.5 μm. A sample of strontium titanate to which 18.25 C of charge was applied developed clumps of triangular crystals with lengths ranging from 1.7 μm-2.0 μm and heights ranging from 0.9 μm-1.1 μm. The sample of strontium titanate that had 60 C of charge applied to it had a large number of densely packed crystals with lengths ranging from 4.9 μm-6.5 μm and heights ranging from 2.8 μm-3.5 μm form upon

its surface. The largest of the charges that was applied to a sample of strontium titanate was that of 98 C. This resulted in the sample being so densely packed with triangular crystals with lengths of 2.4 μm-6.0 μm that the heights of the crystals could not be accurately measured. A summary of the effect of time, potential, and charge can be found in Table 1.

Knowing that applying a positive charge for a certain length of time will result in the formation of the triangular crystals upon the surface of the sample, the question is raised, what is the least that can be done to still cause the triangular crystals to appear. In order to investigate this, samples of strontium titanate were exposed to 1.2 V for various lengths of time. As can be seen in Figure 33, when 1.2 V is applied to the sample for 5 minutes, the triangular crystals do not appear to form upon the surface. Both the area that was submerged in sodium hydroxide and the clipped area feature rounded protrusions on the surface of the sample. The submerged end does have more of these rounded protrusions than the clipped end does. The sample in this case did slightly darken, which is usually indicative of the formation of the triangular crystals upon the strontium titanate's surface. It is possible that the crystals did indeed form upon this sample, but they formed in such small numbers that they just were not present in the areas scanned by atomic force microscopy. The strontium titanate that was exposed to a potential of 1.2 V for 15 minutes was also slightly darkened where the sample was clipped. The investigation using atomic force microscopy did seem to turn up the presence of triangular crystals upon the surface of the sample. As can be seen in Figure 34, the clipped area of the sample does seem to have one triangular crystal on its surface. There do not appear to be any triangular crystals on the surface of the submerged part of the

sample; any crystals that appear to be triangular were found to not be upon closer inspection. However, it should be noted that it is likely that this appearance could just be caused by the tip. It does not appear that any conclusions can be reached about what is the minimum length of time that the potential must be applied in order to cause the triangular crystals to appear. This would require further experimentation in order to determine what minimum length of time would be needed to observe crystal formation.

The next question with regards to how electrochemical modification affects the surface topography of strontium titanate is what effect if any occurs in the area of the sample submerged in sodium hydroxide. Looking at Figure 35, a comparison can be made between the submerged areas of a variety of samples of strontium titanate. The untreated sample featured a large number of bumps on it that were fairly uniformly arranged. Soaking the strontium titanate in sodium hydroxide for 24 hours resulted in a surface with a few large bumps that were uniformly arranged and several smaller bumps that were less uniformly arranged. The sample that was exposed to a potential of 1.0 V for 20 hours had a few bumps of similar size spread out over the surface of the sample with areas of flattened space between them. Exposing the strontium titanate to -1.0 V for 20 hours resulted in a surface containing a few large bumps with a larger number of small bumps arranged randomly. A sample of strontium titanate that was exposed to 0.8 V for 20 hours then exposed to -0.8 V for 20 hours gave a similar result. These are not very large differences between the samples. However, there does appear to be some change taking place upon a finer scale. All of the samples of strontium titanate that were modified in some fashion show features that are larger than that of the unmodified strontium titanate. The largest features on the unmodified strontium titanate have heights

of around 40 nm; this is in comparison to the reduced sample's highest features which had heights of around 120 nm. Therefore, it is necessary to look deeper and compare the average roughness of the samples in order to spot differences. From the graph in Figure 36, it would seem that the sample that was exposed to a potential of -1.0 V was the roughest sample, with the sample that was just soaked in sodium hydroxide being the least rough. The other three samples whose roughness values were measured were similar in terms of average roughness. However, an examination of the standard deviations in average roughness for the samples, as seen in Figure 37, shows that the samples have too great a degree of variation for any judgment to be made on how average roughness varies with regards to treatment.

Changes to Chemical Makeup

As previously mentioned, the triangular crystals that formed upon the surface of the strontium titanate were identified as being rutile titanium dioxide through the use of X-ray diffractometry. The diffraction pattern that shows this can be seen in Figure 38, where a sample of strontium titanate exposed to 1.2 V for 20 hours shows peaks associated with rutile titanium dioxide. This pattern was matched to that which has been observed to form from rutile titanium dioxide. In order to gain a better understanding of the changes that took place during the electrochemical modification of the strontium titanate, the XPS spectra for several of the samples must be examined. The first example that came up for consideration is a sample of strontium titanate that was exposed to 0.65 V for 24.62 hours. The XPS data that was obtained for this sample can be found in Figures 39-41. Looking at the peaks for Ti 2p in Figure 39, it can be seen that there are no major changes for the peaks for the three different areas of the sample. There is a small

shift in binding energy between position 1 and position 2 for the Sr 3d peaks as seen in Figure 40. This could be evidence of the beginnings of the chemical changes that occur to form the titanium dioxide upon the surface of the strontium titanate. This is further backed up by what is seen in Figure 41; the peaks that are caused by the O 1s show an even more noticeable shift between the peaks for position 2 and position 3. This would make sense that moving closer to or further away from the clipped area would result in differences in the types of oxygen or titanium that would be present on the samples surface, such as would result from the formation of titanium dioxide on the surface of the sample.

The next series of XPS spectra up for consideration is that for the strontium titanate that was exposed to 1.0 V for 20 hours as can be seen in Figures 42-44. In Figure 42, the peaks for the Ti 2p again show no major shifts in binding energy for the different positions on the sample. One thing that does stand out on these spectra is that the intensity for the peaks at position 2 are smaller than those for the other positions. Looking at Figure 43, a similar decrease in intensity is seen for the peaks at position 2; in addition to this, there does not seem to be any real shift in binding energy for these Sr 3d peaks. The XPS spectra showing the peaks associated with O 1s also show the decreased peak intensity at position 2 without major shifts in binding energy for the peaks. In order to gain a better understanding of what is going on with this sample, it is beneficial to look at the percentages of the various atomic components present in this sample, as can be seen in Figure 45. From this graph, it can be seen that the percentage of oxygen present is fairly stable for positions 1, 3, and 4, but the percentage of oxygen reaches its highest amount at position 2. Position 2 is on the border of the clipped area; this means that there

is a slight buildup of oxygen on this border position. This increase in the percentage of oxygen is paired with a decrease in the percentage of strontium at the same position. The titanium percentage remains fairly stable throughout this sample.

XPS data has also been collected for samples of strontium titanate that have been exposed to 0.8 V for various lengths of time. The XPS spectra for these samples can be found in Figures 46-49. The Ti 2p peaks of Figure 46 show a very slight shift for when the sample was exposed to 0.8 V for all the lengths of time relative to the unmodified sample; in addition to this there is a slight decrease in peak intensity for the samples exposed to 0.8 V for 0.5 hours, 2 hours, and 4 hours relative to the unmodified sample and that exposed for 6 hours. As can be seen in Figures 47 and 48, a similar pattern is true for the O 1s peaks and the Sr 3d peaks. The peaks for O 1s do show something unusual for the sample exposed to 0.8 V for 0.5 hours; the shoulder-like peak seems to have broken up into two different peaks. The peaks caused by C 1s seen in Figure 49 do not seem to follow any set pattern. This is expected, since the carbon peaks are caused by carbonate contamination. Looking at the percentage of the atomic components found in Figure 50, a pattern can be seen. The atomic percentage of oxygen reaches its highest amount for the sample exposed to 0.8 V for 0.5 hours before decreasing as the length of time exposed increases. This continues to the point that the oxygen percentage is lower at the 6 hour mark than it is for the unmodified strontium titanate. For the strontium, the percentage decreases going from unmodified sample to the 0.5 hour mark. After that, the percent of strontium present increases back to the same level as the unmodified sample after being exposed to 0.8 V for 2 hours. The samples that were exposed for 4 hours and 6 hours both have a slight increase in percentage of strontium relative to the sample

exposed for 2 hours. The atomic percentage of titanium present holds steady when comparing unmodified strontium titanate to that exposed to 0.8 V for 0.5 hours. An exposure to the same potential for 2 hours causes a slight decrease in the percentage of titanium. The longer exposures of 4 hours and 6 hours are accompanied by a fairly steady increase in the percentage of titanium present.

These results point to something happening with regards to the oxygen present on the modified samples of strontium titanate. The X-ray diffraction data shows that titanium dioxide crystals formed upon the surface of the modified strontium titanate. This would certainly be a different form of oxygen relative to that of the strontium titanate, which could explain the changes noticed for the O 1s peaks.

Removing the Crystals

During the course of this research, methods of how to remove the crystals of titanium dioxide from the surface of the strontium titanate were investigated. The first method of removing the crystals that was investigated involved applying a negative potential of similar magnitude to a sample that had previously had a positive potential applied to it; the results of this can be seen in Figure 51. As can be seen, the negative potential does not appear to have any effect upon the triangular crystals. The number of the crystals, the density of their packing, and the size of the crystals remains unchanged between the two samples.

An actual method that was found to be successful for removing the crystals was discovered during the course of cleaning excess sodium hydroxide off of a sample. By sonicating the electrochemically modified sample of strontium titanate in water, it was found that the crystals of titanium dioxide could be removed from the sample. A sample

that was exposed to 1.2 V for 20 hours and then sonicated in water was found to be less dark on the clipped end after sonication than it was before sonication. The results of AFM scans on the sample bear this out; looking at Figure 52, it can be seen that there is a marked difference between a sample that was sonicated and a sample that was not sonicated even though the samples were exposed to the same potential for the same length of time. This provides evidence that the titanium dioxide is somewhat loosely held to the surface of the strontium titanate.

Potential Model for Changes

Another question that arises from these results is why do they occur? In order to explain this, a model has been proposed; this model can be seen illustrated in Figure 53. What could be occurring is that when the oxygen species is absorbed into the strontium titanate from the sodium hydroxide, it travels up the strontium titanate under the influence of the electric current. When the oxygen species reaches the clipped area, it can go no further, and it is here where the oxygen species reacts with the strontium titanate to produce titanium dioxide. This does fit with what is known about the circumstances under which the crystals form. Only a positive potential would cause the oxygen species to be incorporated and move to the correct area; the negative potential would not have the electric field going in the right direction for the change to occur. Further evidence of this is found in that applying a negative potential to a sample that has already been exposed to a positive potential does not cause the triangular crystals to be removed. The change has already occurred to the strontium titanate, and there is no way for the negative potential to change this because of the way that the electric field is going. However, further research will need to be done in order to determine if this is indeed the mechanism for

this change.

For instance, carrying out the electrochemical modification under argon or nitrogen could eliminate the possibility that the oxygen is somehow being incorporated from the air. In addition to this, kinetic and thermodynamic studies could help to determine the nature of the reaction taking place.

Potential Uses of the Changes

Now that it is possible to place the titanium dioxide upon the surface of the strontium titanate, the question that is asked is what can this be used for? It is known that titanium dioxide can be used as a photocatalyst for a variety of reactions, one of which is the breakdown of water into hydrogen and oxygen.[22] A model for how this could be used is seen in Figure 54. This method could be used to generate hydrogen gas for use in fuel cells, a more green form of energy than the current use of gasoline and diesel. In addition to this, this would allow the production of hydrogen from water to be powered by naturally occurring light, a renewable source of energy. Another advantage that this method has is that the titanium dioxide is placed upon a substrate in the process of altering the strontium titanate; this means that the titanium dioxide is ready to use in the system.

Another type of reaction for which titanium dioxide can act as a photocatalyst is the breakdown of organic waste, such as the dye polluted run-off from textile factories, into more environmentally friendly products.[23] The set up for which this can be used that is seen in Figure 55 shares many of the advantages of the set up in Figure 54. The breakdown is powered by naturally occurring light, and the titanium dioxide is already deposited on the surface of the substrate, ready to be used in the set up. This would be of

enormous benefit to the environment by reducing the amount of pollution that could be released into the water. Future research will need to be done to see how easily this method can be scaled up in order to make industrial size versions of the titanium dioxide deposited upon the surface of strontium titanate substrates.

One major drawback to the use of this method is that neither reaction relies upon the titanium dioxide being present upon a strontium titanate substrate. However, titanium dioxide upon a strontium titanate substrate has been shown to be hydrophilic when exposed to UV light and hydrophobic when exposed to visible light. This would allow for water to be reversibly stored upon a surface of titanium dioxide on a strontium titanate substrate. The method that was used in the literature to obtain the titanium dioxide on the strontium titanate was organometallic chemical vapor deposition.[24] This method requires the deposition to occur at elevated temperatures and uses a complicated set-up.[25] The electrochemical modification method allows for the placing of titanium dioxide upon the surface of strontium titanate at room temperature using a relatively simple set-up.

Additional Considerations for Future Research

One area in which future research will need to be done is in the area of directed growth. It would be of great benefit to see if it is possible to alter where the titanium dioxide crystals will appear upon the surface of the strontium titanate by altering where the alligator clip is placed upon the surface of the sample. Another area for future research relates to the use of strontium titanate as an oxygen detector. The results of this research prove that it is possible for strontium titanate to be altered under the right conditions. It might be possible that environmental conditions could cause alterations to the strontium titanate that is used in oxygen detectors as well. This could alter the results

obtained from using an oxygen detector, and as such would be worth looking into in order to make sure that this would not happen to such a level as to negatively affect the operations of an oxygen detector. In addition to this, a look at what effect the electrochemical modification has upon the surface topography of strontium titanate upon a much finer scale should be taken.

Conclusions

The goal of this research was to study what effects electrochemical modification would have upon the surface topography of samples of strontium titanate and upon the chemical makeup of the strontium titanate. In order to investigate these changes, atomic force microscopy and XPS spectroscopy were used. It was found that a positive potential being applied to a sample of strontium titanate for a long enough period would result in the formation of triangular crystals upon the surface of the strontium titanate where the sample was clipped. It was also found that increasing the potential applied to the sample or the time for which the potential was applied would generally result in the formation of larger, more numerous, and more densely packed triangular crystals. These crystals were found to be impossible to remove by applying a negative potential to the sample, but were found to be loosely held enough that sonication of the samples could remove the crystals. These crystals were identified as being titanium dioxide, a material that can be used as a photocatalyst. As such, the method discovered in the course of this research shows potential as a method for preparing materials that could be of enormous use in the production of hydrogen, a green energy source, and the treatment of run-off from factories, a method that could reduce pollution. The experimental investigation into the electrochemical properties of strontium titanate brought to light factors that may be of issue for lengthy modification of strontium titanate and for optimizing the results.

References

1. Lytle, F. W. *J. Appl. Phys.* **1964,** *35,* 2212-2215.

2. Colored Gemstones Guide. http://www.gemstones-guide.com/Strontium-Titanate.html (accessed 2/25/13).

3. Szot, K.; Speier, W. *Phys. Rev. B.* **1999**, *60*, 5909-5926.

4. Grenier, J. C.; Wattiaux, A.; Fournes, L.; Pouchard, M.; Etourneau, J. *J. Phys. IV France.* **1997**, *7*, 49-52.

5. Merkle, R.; Maier, J. *Angew. Chem. Int. Ed.* **2008,** *47,* 3874-3894.

6. Merkle, R.; Maier, J. *Phys. Chem. Chem. Phys.* **2002**, *4*, 4140 –4148.

7. Pecchi, G.; Jiliberto, G. M.; Delgado, E. J. *J. Chil. Chem. Soc.* **2011**, *56*, 895-900.

8. Martynczuk, J.; Liang, F.; Arnold, M.; Šepelák, V.; Feldhoff, A. *Chem. Mater.* **2009**, *21*, 1586-1594.

9. Garg, K. B.; Gaur, S. K.; Singhal. R. K. Pal, P.; Sekhar, B. R.; Nordblad, P.; Carlson, S. *Int. J. Mod. Phys. B.* **2010**, *24*, 2135-2148.

10. Morandat, S.; Azouzi, S.; Beauvais, E.; Mastouri, A.; El Kirat, K. *Anal. Bioanal. Chem.* **2013**, *405*, 1445-1461.

11. Li, M.; Xiao, X.; Liu, L.; Xi, N.; Wang, Y.; Dong, Z.; Zhang, W. *Scanning.* **2013**, *35*, 40-46.

12. Wojtyniak, M.; Szot, K.; Wrzalik, R.; Rodenbücher, C.; Roth, G.; Waser, R. *J.*

Appl. Phys. **2013**, *113*, 083713.

13. Ron Reifenberger (2010), "ME 597 Lecture 4: The Transition from STM to AFM," https://nanohub.org/resources/9685. (accessed 3/5/13).

14. Binnig, G.; Quate, C. F. *Phys. Rev. Lett.* **1986**, *56*, 930-933.

15. Ron Reifenberger (2010), "ME 597 Lecture 5: Interaction Forces I," https://nanohub.org/resources/9713. (accessed 3/5/13).

16. NT-MDT. http://www.ntmdt.com/ (accessed 3/5/13).

17. Arvind Raman (2010), "ME 597 Lecture 14: Introduction to Dynamic AFM," https://nanohub.org/resources/9955. (accessed 3/5/13).

18. Richard J. Matyi; NCLT administator (2008), "Modern X-ray Scattering Methods for Nanoscale Materials Analysis," https://nanohub.org/resources/5580. (accessed 4/6/13).

19. Dmitry Zemlyanov (2007), "Introduction to X-ray Photoelectron Spectroscopy and to XPS Applications," https://nanohub.org/resources/2668. (accessed 4/6/13).

20. van der Heide, P. A. W.; Jiang, Q. D.; Kim, Y. S.; Rabalais, J. W. *Surface Science*, **2001**, *473*, 59-70.

21. Sadeghi, F. https://engineering.purdue.edu/ME556 (accessed 3/26/13).

22. Chen, X.; Liu, L.; Yu, P. Y.; Mao, S. S. *Science*, **2011**, *331*, 746-750.

23. Konstantinou, I. K.; Albanis, T. A. *Applied Catalysis B: Environmental*, **2004**, *49*,

1-14.

24. Miyauchi, M.; Kieda, N.; Hishita, S.; Mitsuhashi, T.; Nakajima, A.; Watanabe, T.; Hashimoto, K. *S. Science,* **2002**, *551*, 401-407.

25. Coleman, J. J. *Proc. IEEE,* **1997**, *85*, 1715-1729.

Appendix A:

Figures from the Results Section and Captions

Figure 15: Picture of strontium titanate sample exposed to positive potential. The darkened area is where the sample was clipped to serve as a working electrode.

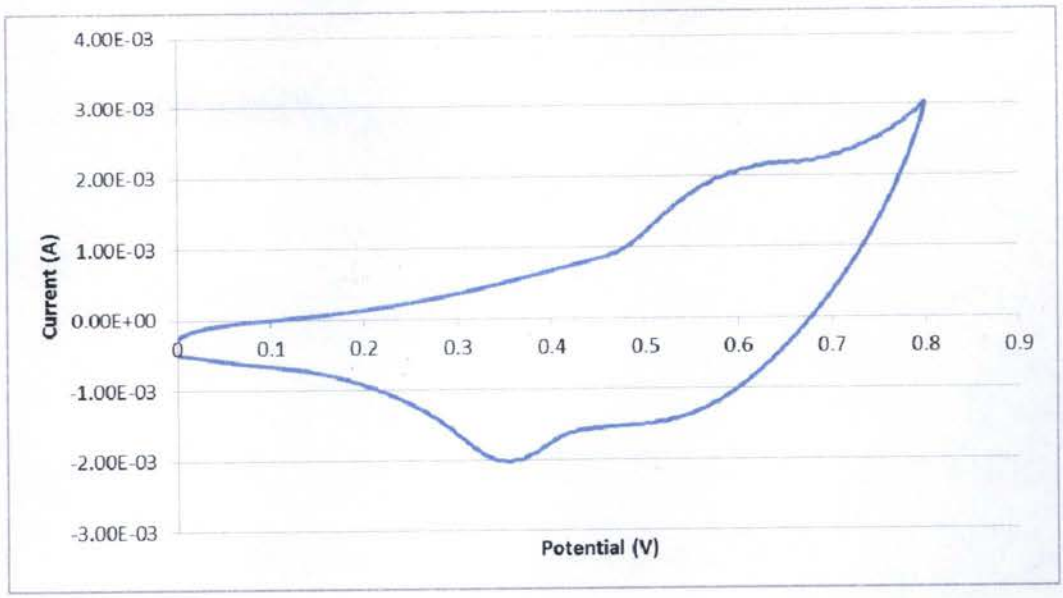

Figure 16: Cyclic voltammogram of strontium titanate in 1 M NaOH with a scan rate of 50 mV/s.

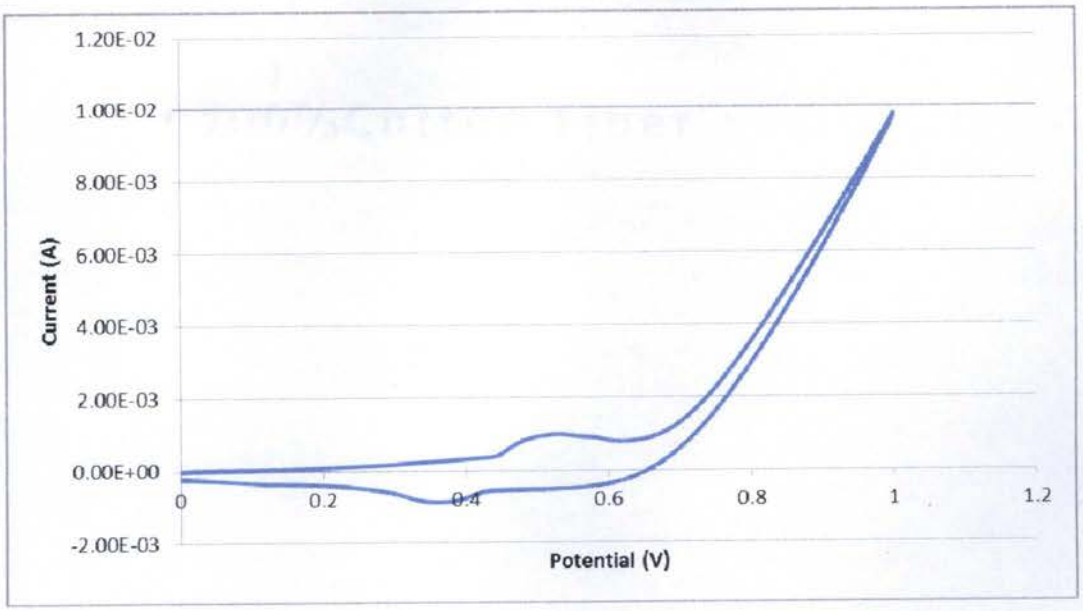

Figure 17: Cyclic voltammogram of strontium titanate in 1 M NaOH with a scan rate of 50 mV/s.

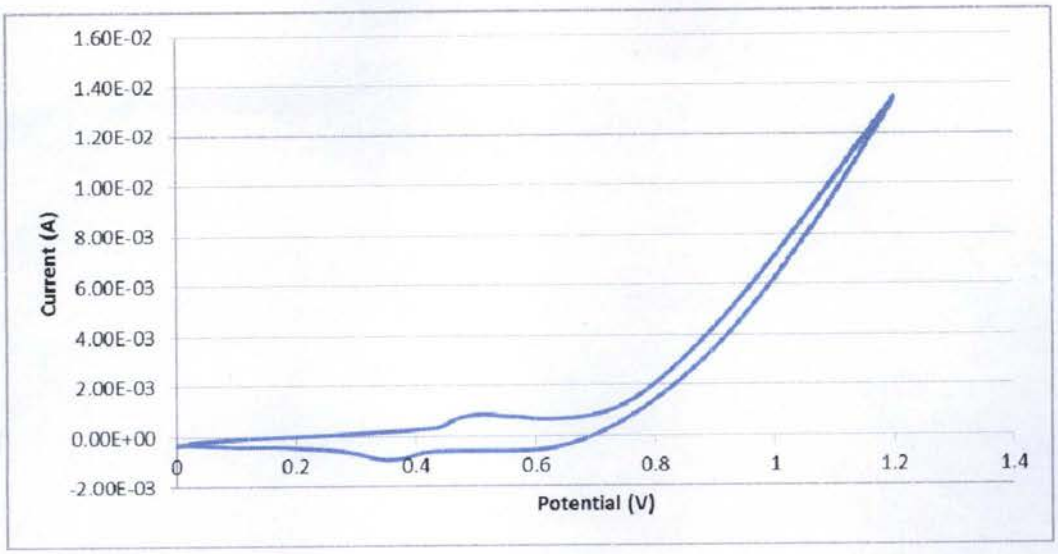

Figure 18: Cyclic voltammogram of strontium titanate in 1 M NaOH with a scan rate of 50 mV/s.

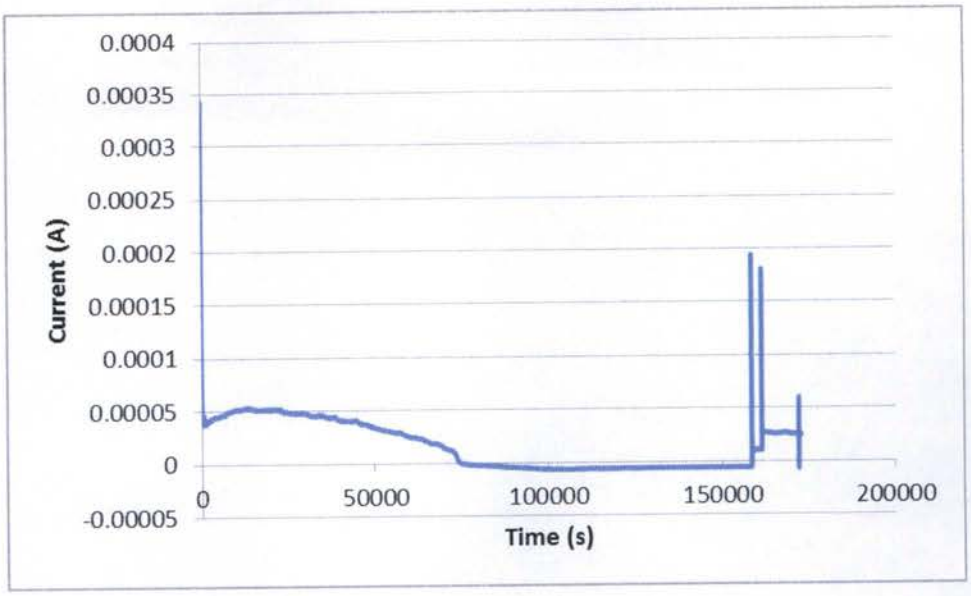

Figure 19: Amperometric i-t curve for electrochemical oxidation of strontium titanate where evaporation causes the working electrode to lose contact with the electrolyte. Current spikes occurred when sample was pushed back into the electrolyte.

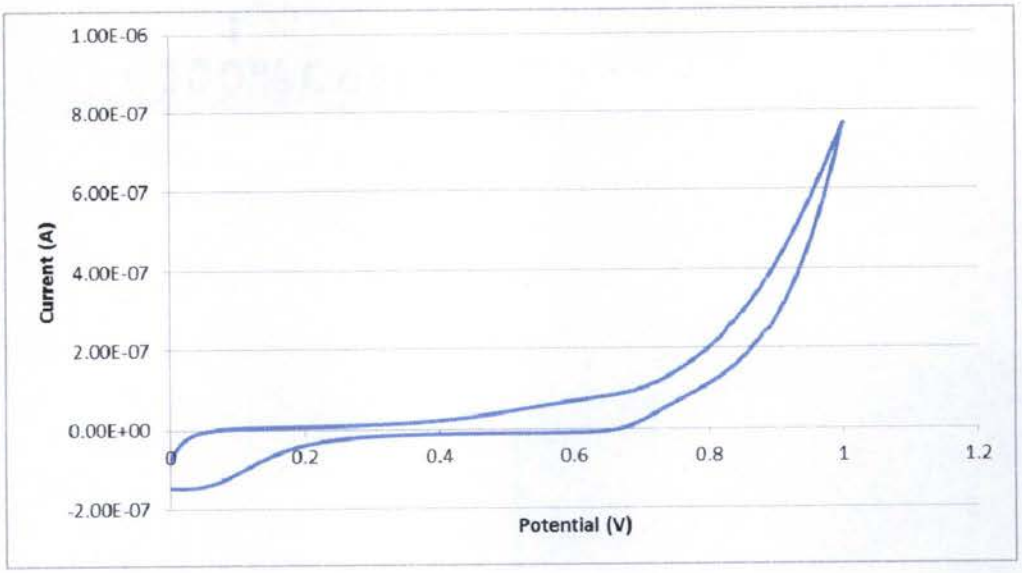

Figure 20: Cyclic voltammogram where reference electrode is moved so as to be adjacent to the working electrode. The voltammogram was taken in 1 M NaOH at a scan rate of 50 mV/s.

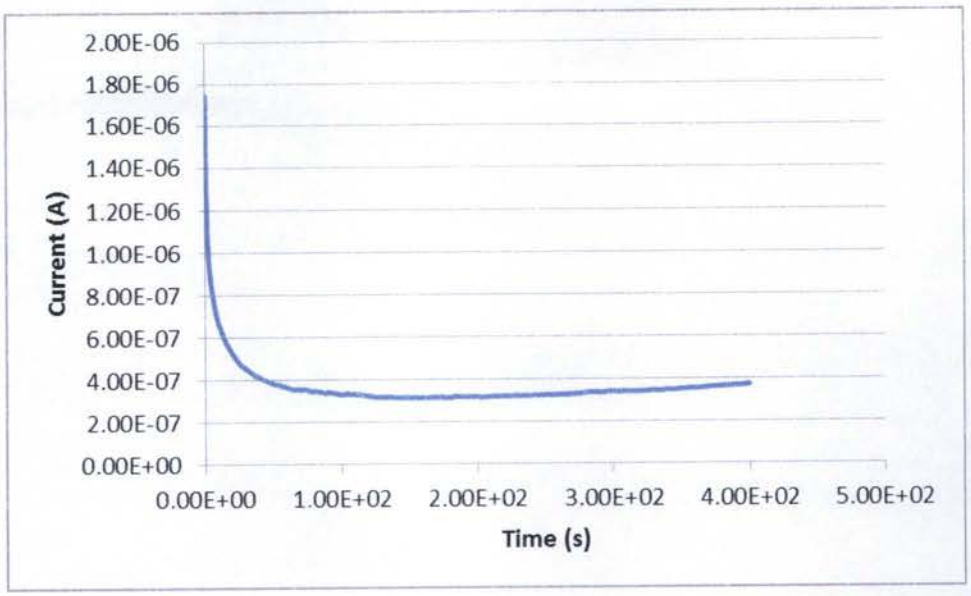

Figure 21: Amperometric i-t curve at 1.0 V where reference electrode is moved so as to be adjacent to the working electrode.

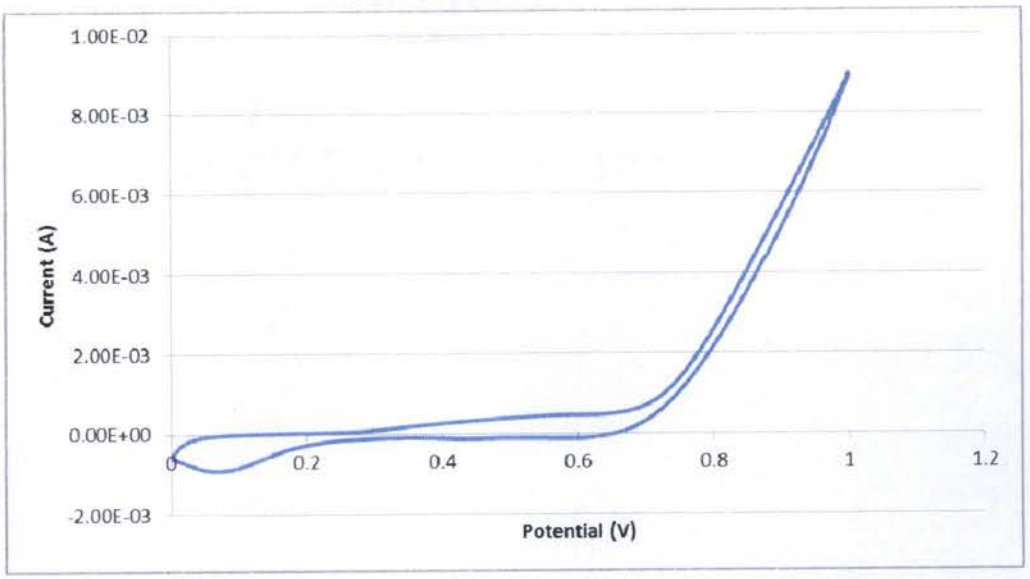

Figure 22: Cyclic voltammogram where reference electrode and working electrode are held at fixed positions by three-pronged clamps.

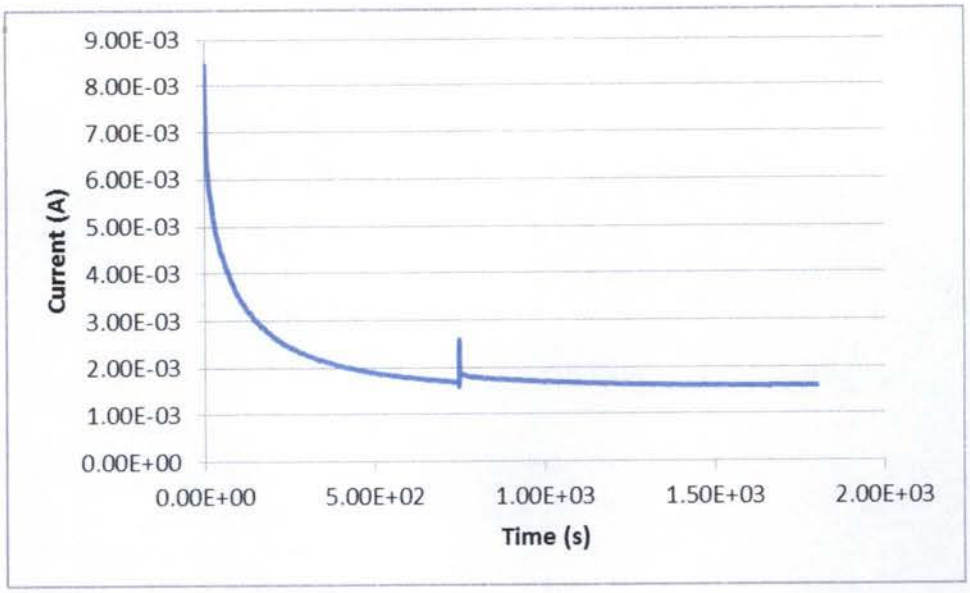

Figure 23: Amperometric i-t curve at 1.0 V where reference electrode and working electrode are held at fixed positions by three-pronged clamps.

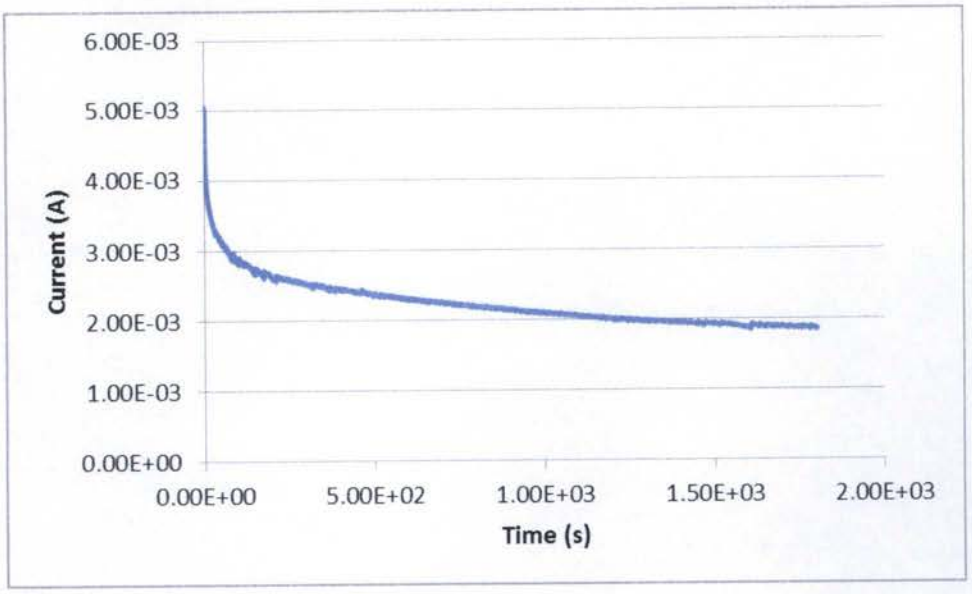

Figure 24: Amperometric i-t curve at 1.2 V where reference electrode and working electrode are held at fixed positions by three-pronged clamps.

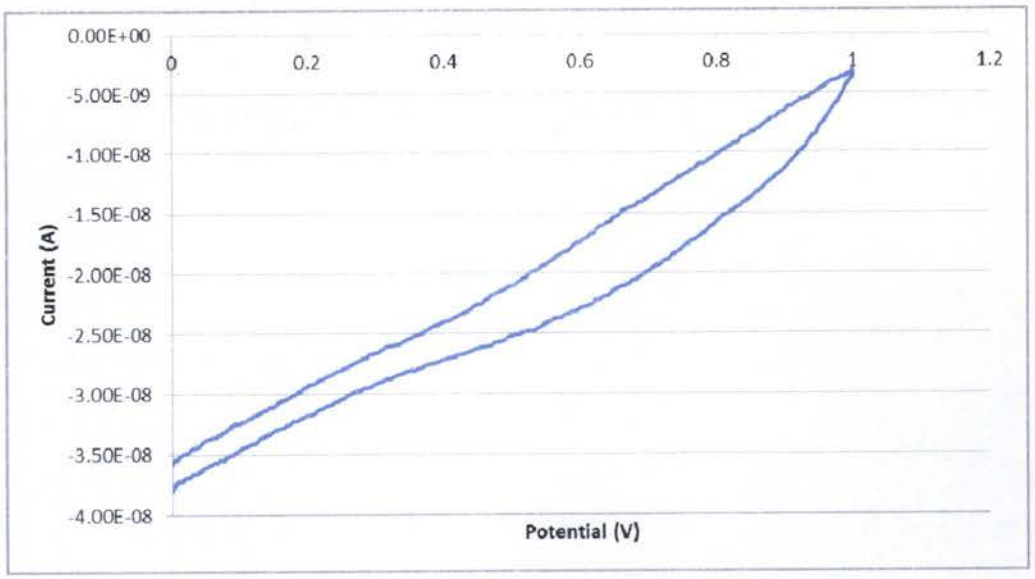

Figure 25: Cyclic voltammogram showing effect of badly corroded electrode leads.

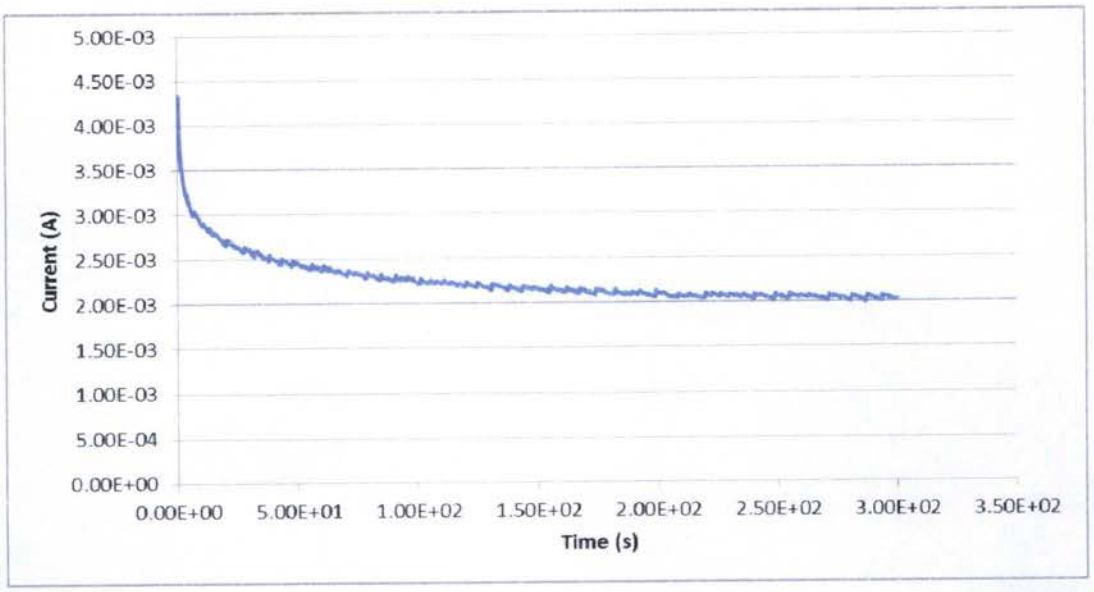

Figure 26: Amperometric i-t curve at 1.2 V showing effect of new electrode leads.

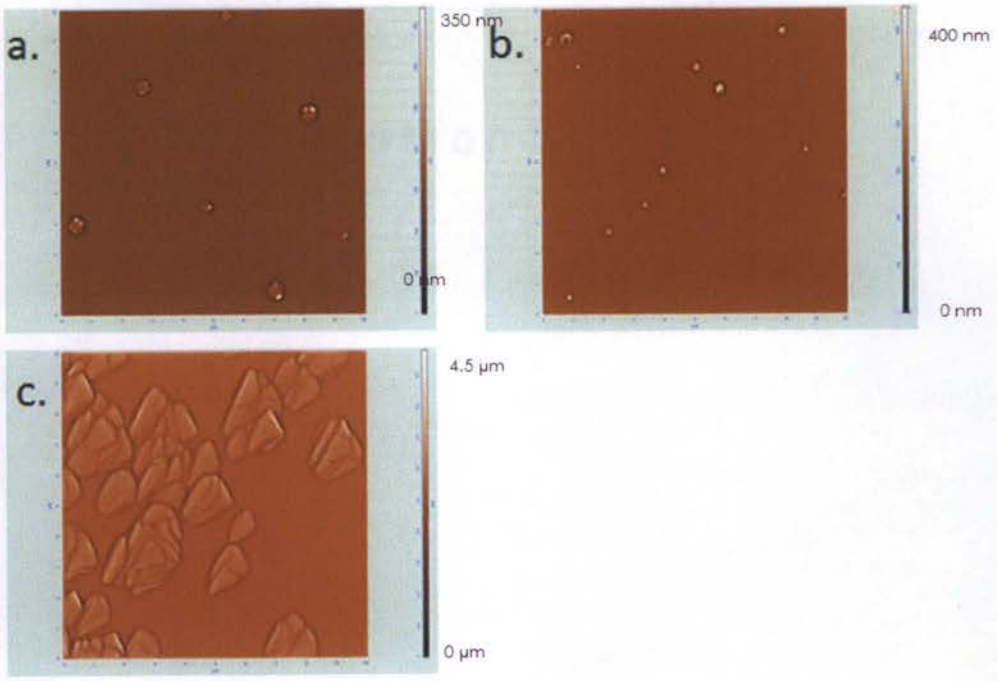

Figure 27: All micrographs are 10 µm x 10 µm and are taken from the clipped area using semicontact mode using tips with a resonance frequency of 300 kHz.. a.) Untreated strontium titanate b.) Strontium titanate exposed to -1.0 V for 20 hours c.) Strontium titanate exposed to 1.2 V for 1.27 hours.

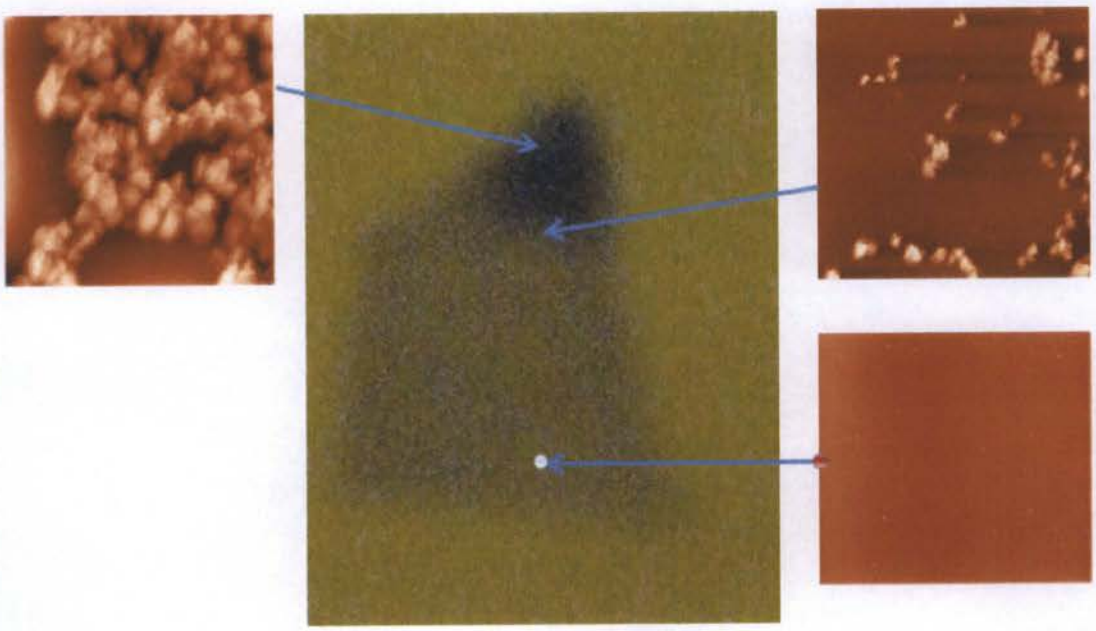

Figure 28: Diagram showing that the triangular crystals only appear upon the clipped end of the strontium titanate and not on the submerged end.

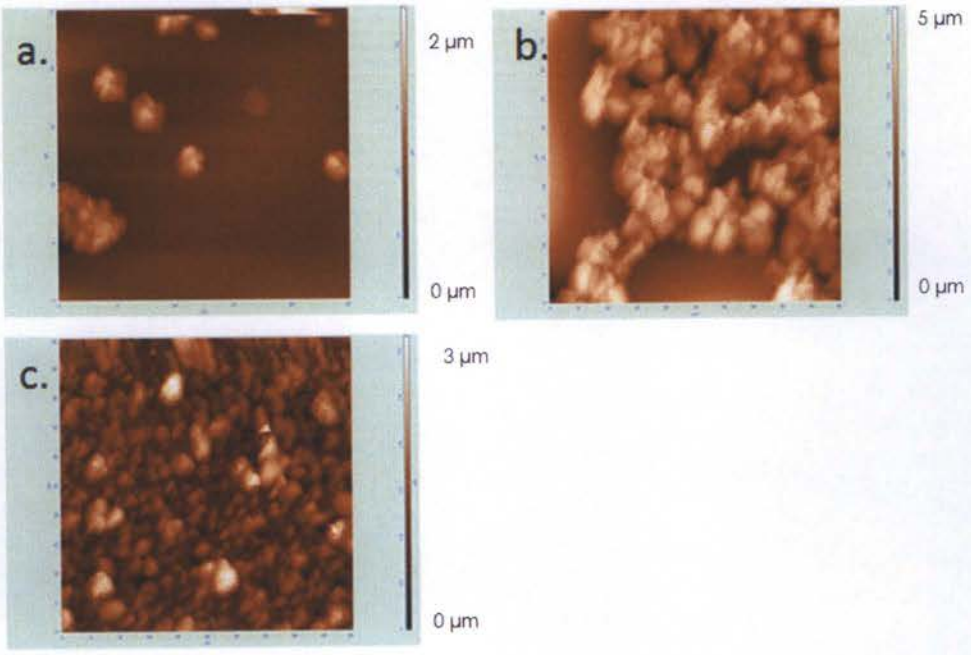

Figure 29: All micrographs are 50 µm x 50 µm and are taken from the clipped area. Micrographs were produced using semicontact mode with tips that had resonance frequencies of 300 kHz. a.) Strontium titanate exposed to 0.8 V for 20 hours b.) Strontium titanate exposed to 1.0 V for 20 hours c.) Strontium titanate exposed to 1.2 V for 20 hours.

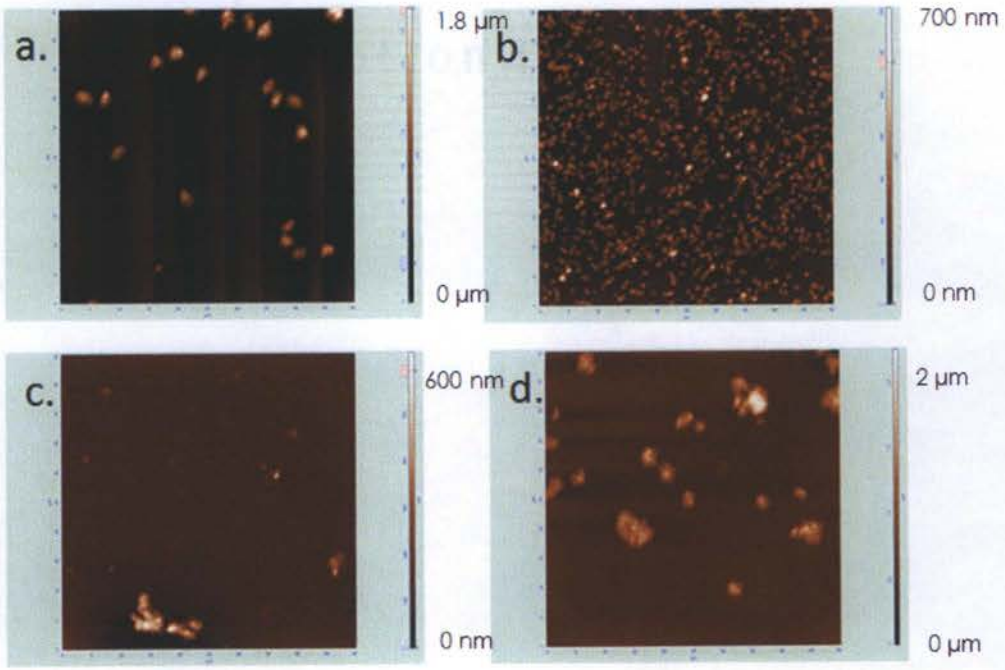

Figure 30: All micrographs are 50 µm x 50 µm and are taken from the clipped areas. Micrographs were produced using semicontact mode with tips that had resonance frequencies of 300 kHz. a.) Strontium titanate exposed to 0.8 V for 2 hours b.) Strontium titanate exposed to 0.8 V for 4 hours c.) Strontium titanate exposed to 0.8 V for 6 hours d.) Strontium titanate exposed to 0.8 V for 20 hours.

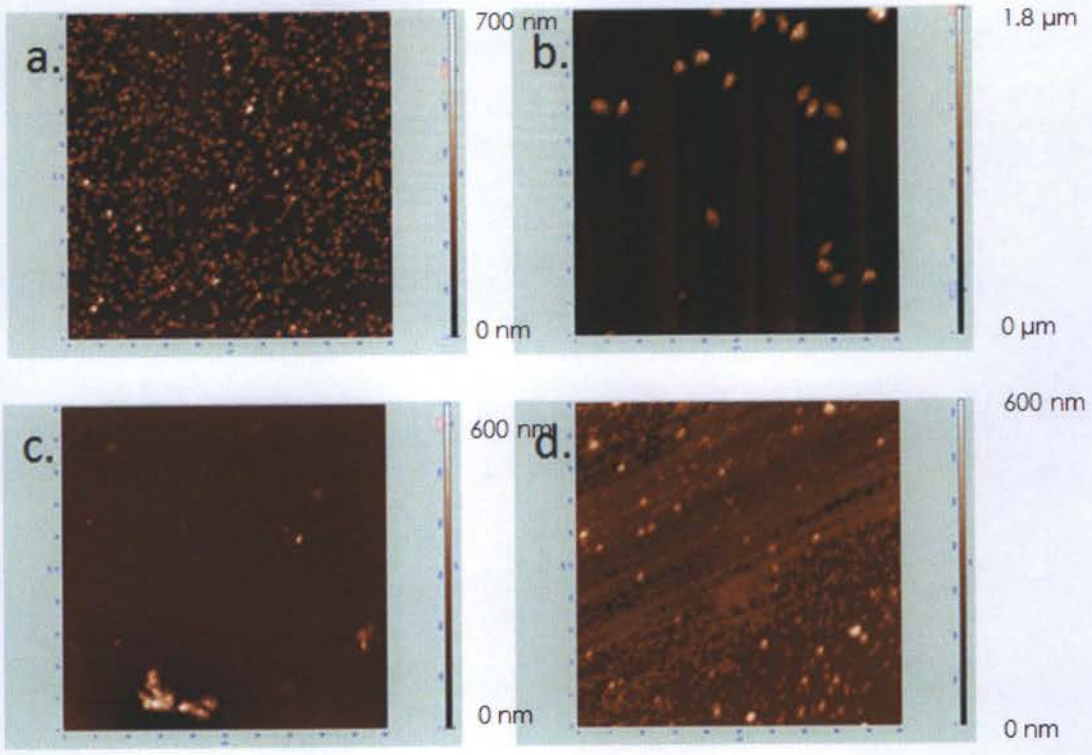

Figure 31: All micrographs are 50 µm x 50 µm and are taken from the clipped ends. Micrographs were produced using semicontact mode with tips that had resonance frequencies of 300 kHz. a.) Strontium titanate to which 0.689 C has been applied b.) Strontium titanate to which 1.25 C has been applied c.) Strontium titanate to which 5.4 C has been applied d.) Strontium titanate to which 10.75 C has been applied.

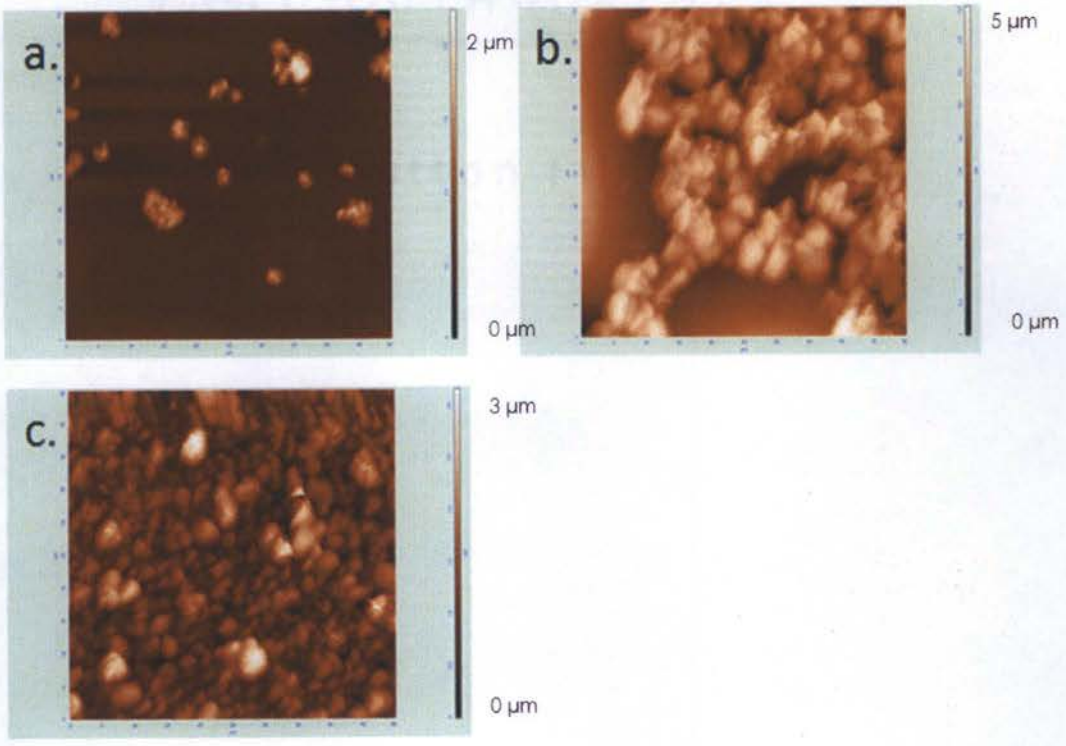

Figure 32: All micrographs are 50 µm x 50 µm and are taken from the clipped ends. Micrographs were produced using semicontact mode with tips that had resonance frequencies of 300 kHz. a.) Strontium titanate to which 18.25 C has been applied b.) Strontium titanate to which 60 C has been applied c.) Strontium titanate to which 98 C has been applied.

STO Sample	Time (h)	Potential (V)	Color	Charge (C)	Range of Crystal Heights	Range of Crystal Lengths
7	4	0.8	Very slightly darkened	.689	300 nm-350 nm	~1.0 μm
6	2	0.8	Light grey	1.25	0.6 μm-1.2 μm	2.3 μm-3.0 μm
11	6	0.8	Darkened along edge	5.4	16 nm-23 nm	0.5 μm-1.0 μm
12	1.27	1.2	Darkened (small areas of black along edges)	10.75	~200 nm	0.6 μm-1.5 μm
5	20	0.8	Grey	18.25	0.9 μm-1.1 μm	1.7 μm-2.0 μm
1	20	1	Dark grey (almost black in parts)	60	2.8 μm-3.5 μm	4.9 μm-6.5 μm
13	20	1.2	Black in parts	98	Cannot be measured	2.4 μm-6.0 μm

Table 1: Summary of the effects of time, potential, and charge upon the surface topography of electrochemically modified strontium titanate.

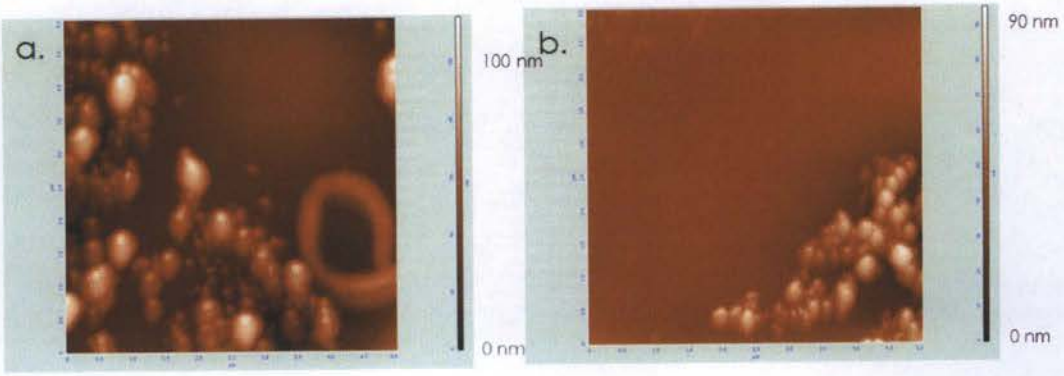

Figure 33: All micrographs are 5 μm x 5 μm and are taken from a sample of strontium titanate exposed to 1.2 V for 5 minutes. Micrographs were produced using semicontact mode with tips that had resonance frequencies of 240 kHz. a.) Micrographs taken from the submerged end of the sample. b.) Micrograph taken from the clipped end of the sample.

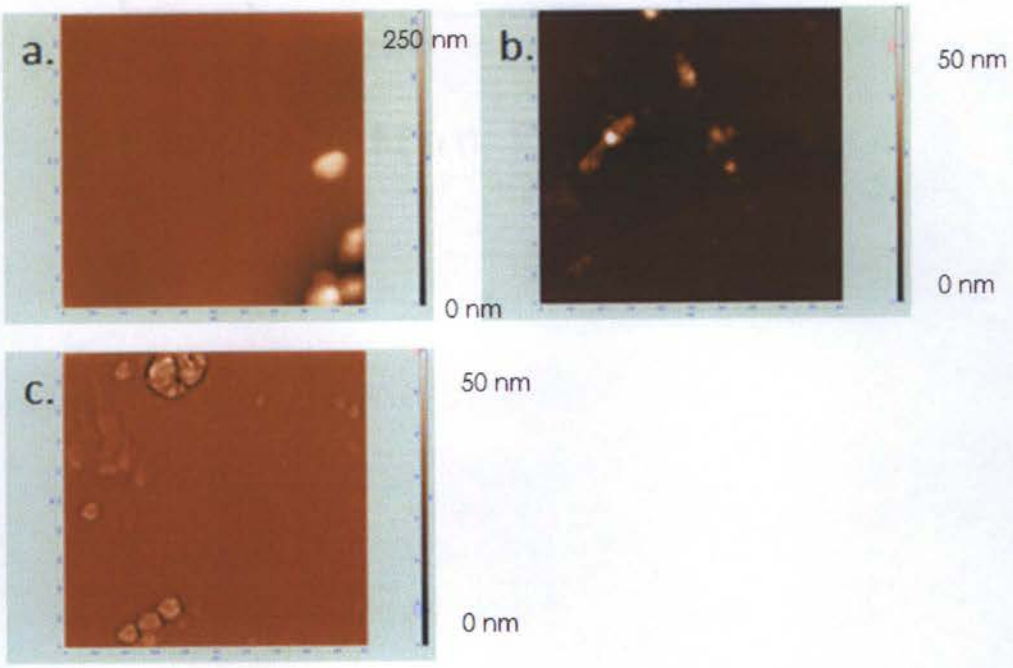

Figure 34: All micrographs are taken from the strontium titanate exposed to 1.2 V for 15 minutes. Micrographs were produced using semicontact mode with tips that had resonance frequencies of 240 kHz. a.) Micrographs taken from the clipped end showing what appears to be one triangular crystal. Micrograph is 5 μm x 5 μm. b.) Micrographs taken from the submerged end; micrograph is 5 μm x 5 μm. c.) Micrographs taken from the submerged end showing crystals from part b at a higher magnification; micrograph is 2 μm x 2 μm.

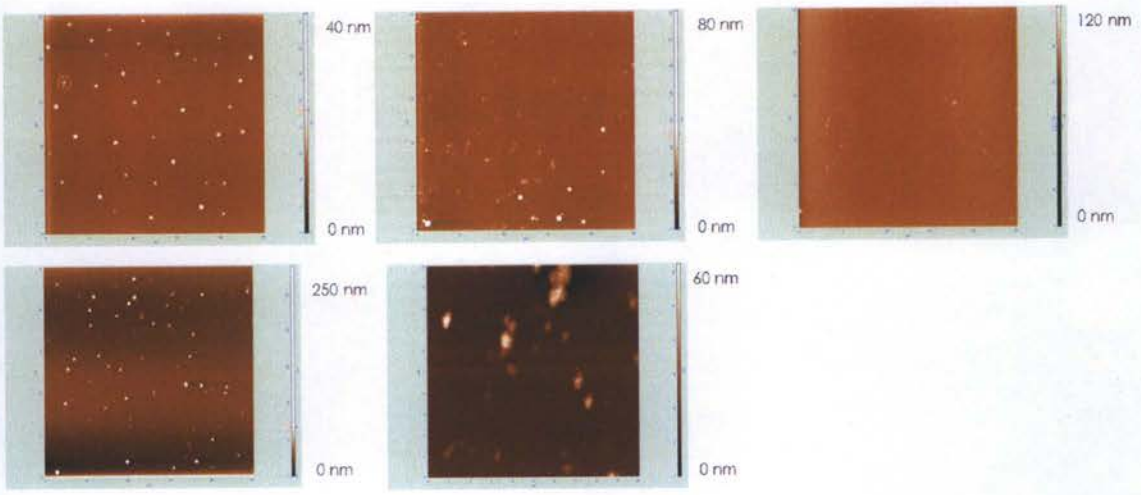

Figure 35: All micrographs are 50 μm x 50 μm and are taken from the submerged ends. Micrographs were produced using semicontact mode with tips that had resonance frequencies of 240 kHz. a.) Untreated strontium titanate b.) Strontium titanate soaked in 1 M sodium hydroxide for 24 hours c.) Strontium titanate exposed to 1.0 V for 20 hours d.) Strontium titanate exposed to -1.0 V for 20 hours e.) Strontium titanate exposed to 0.8 V for 20 hours then exposed to -0.8 V for 20 hours.

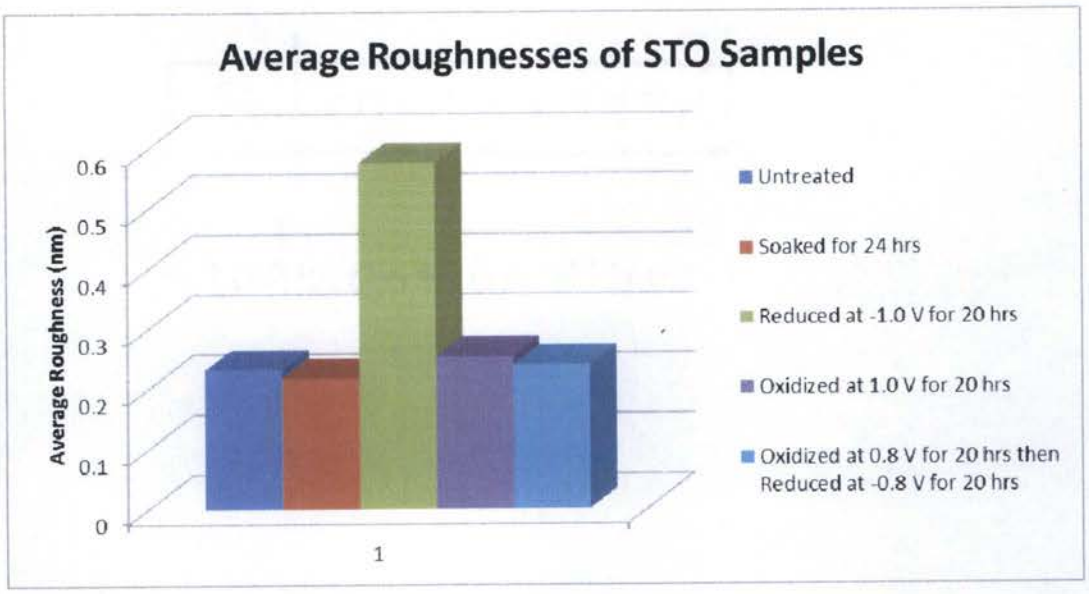

Figure 36: Graph showing variance of average roughness of submerged end of strontium titanate with regards to treatment.

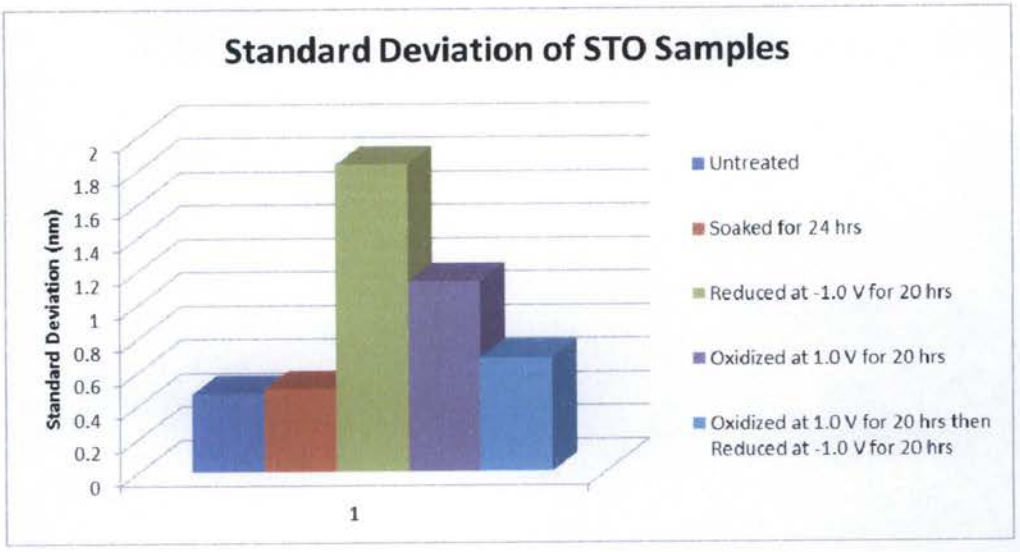

Figure 37: Graph showing how standard deviation of average roughness varies with regards to the treatment of the sample.

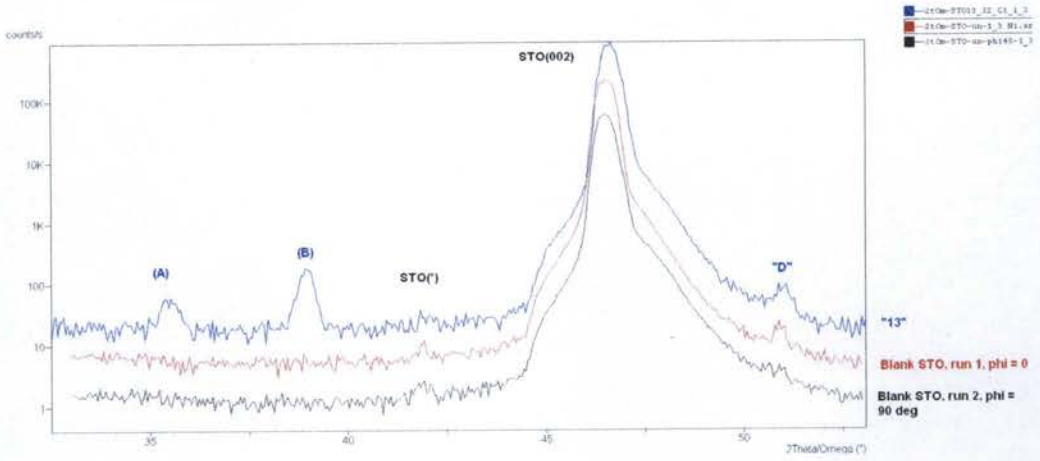

Figure 38: X-ray diffraction spectrum for two unmodified samples of strontium titanate and one sample exposed to 1.2 V for 20 hours (labeled as 13). Peaks A and B for 13 are caused by the presence of rutile titanium dioxide. The peak labeled D is likely caused by the substrate.

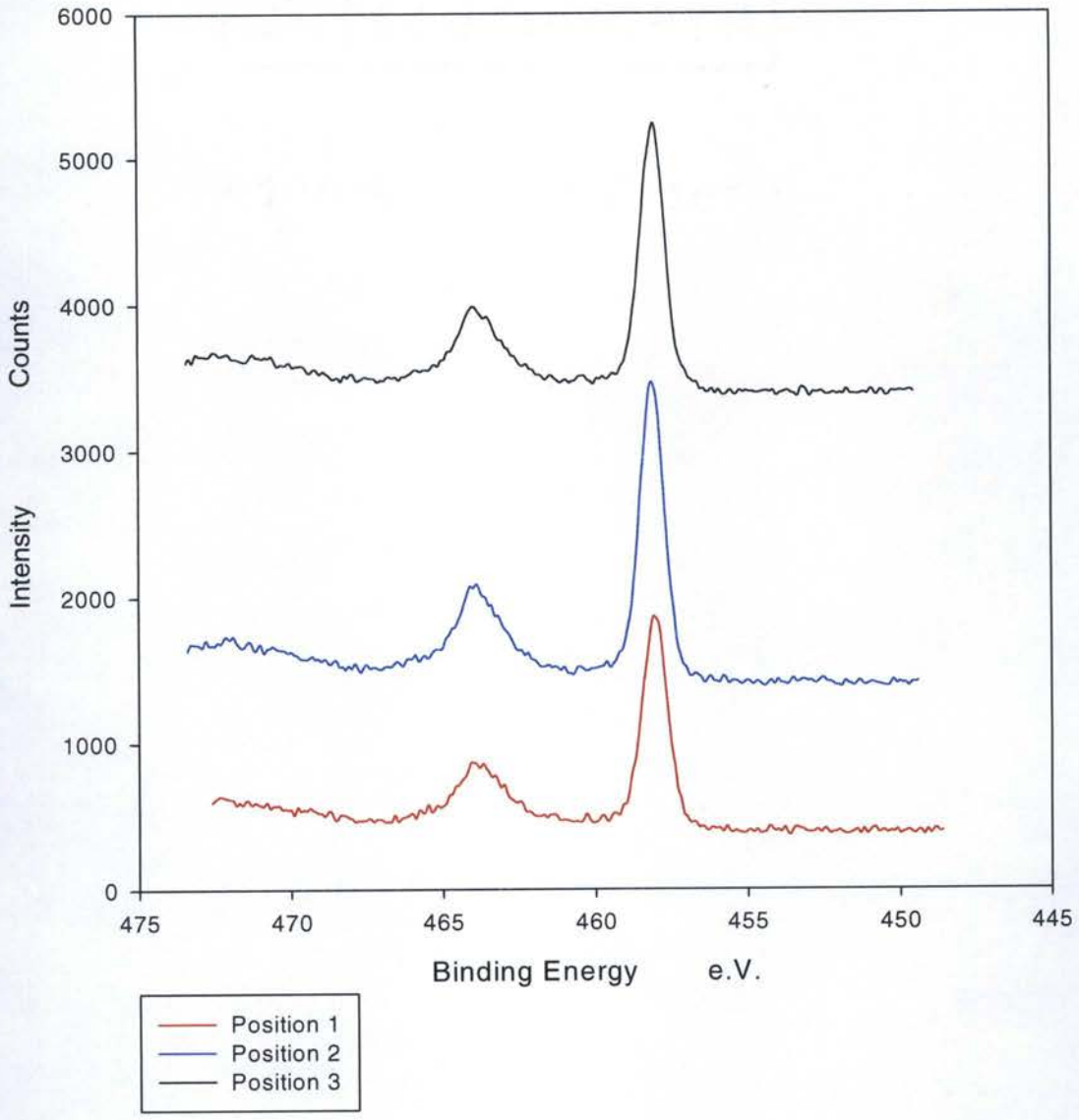

Figure 39: XPS spectra showing the Ti 2p peaks for a sample of strontium titanate exposed to 0.65 V for 24.62 hours. The positions start on the clipped end and move away from there.

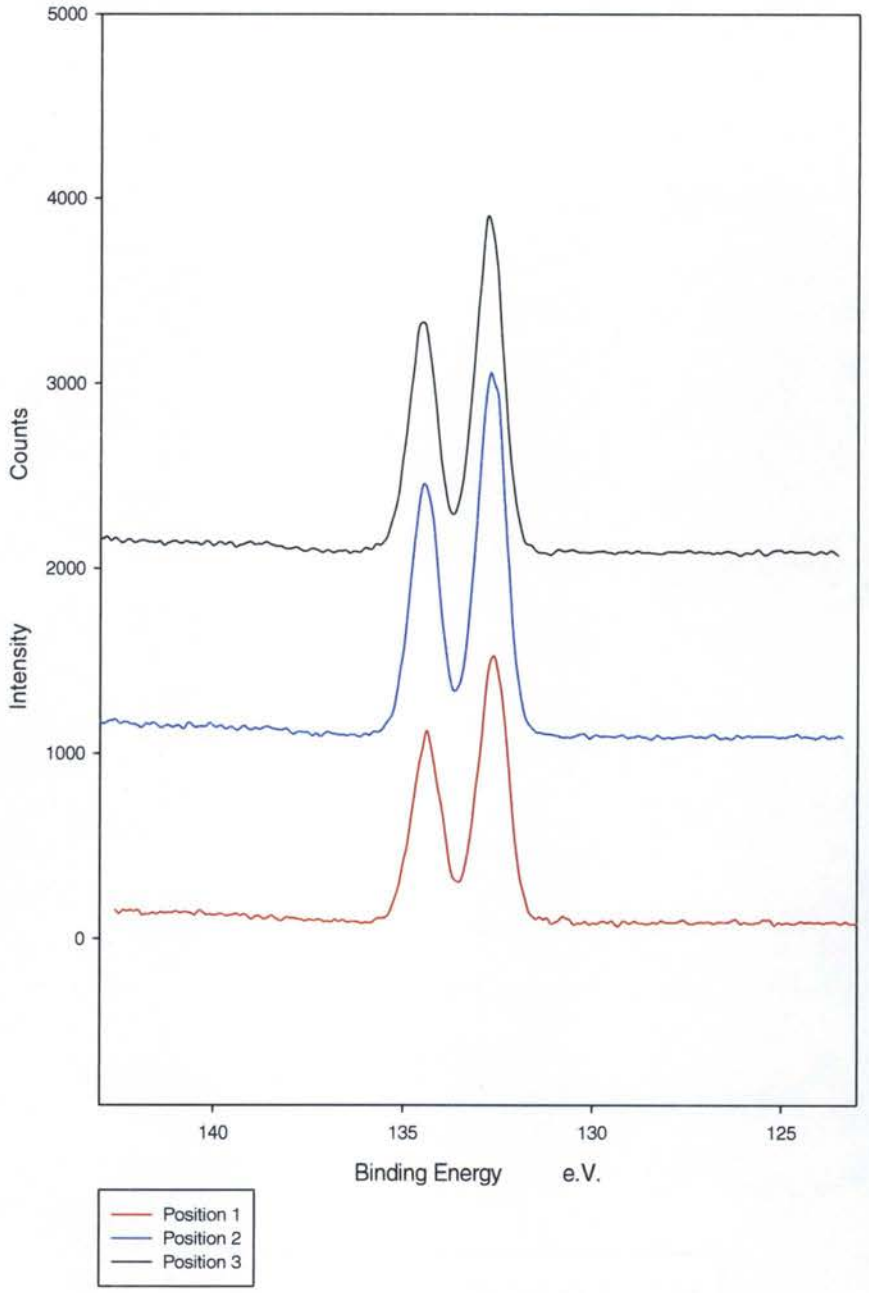

Figure 40: XPS spectra showing the Sr 3d peaks for a sample of strontium titanate exposed to 0.65 V for 24.62 hours. The positions start on the clipped end and move away from there.

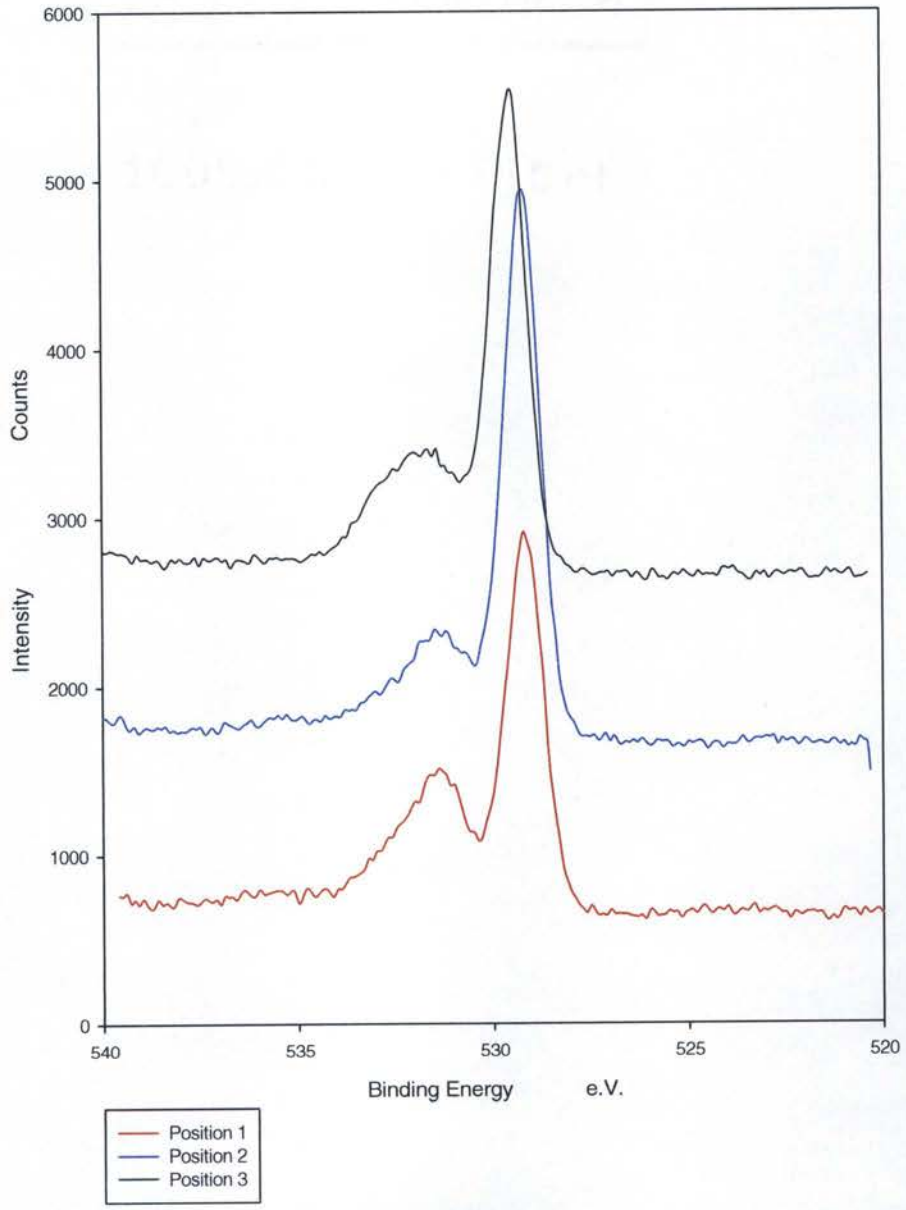

Figure 41: XPS spectra showing the O 1s peaks for a sample of strontium titanate exposed to 0.65 V for 24.62 hours. The positions start on the clipped end and move away from there.

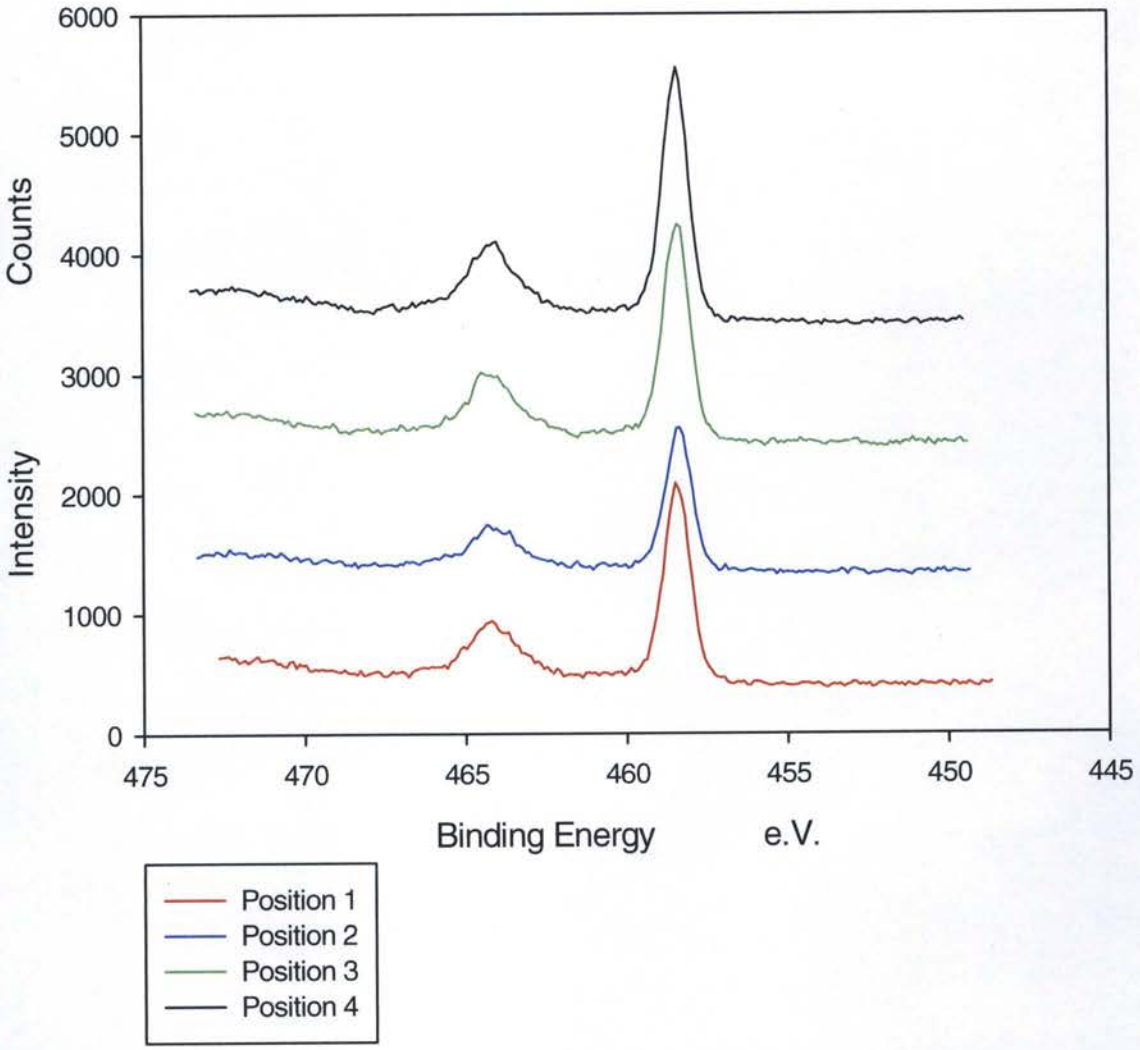

Figure 42: XPS spectra showing the Ti 2p peaks for a sample of strontium titanate exposed to 1.0 V for 20 hours. The positions start on the clipped end and begin to move away from it.

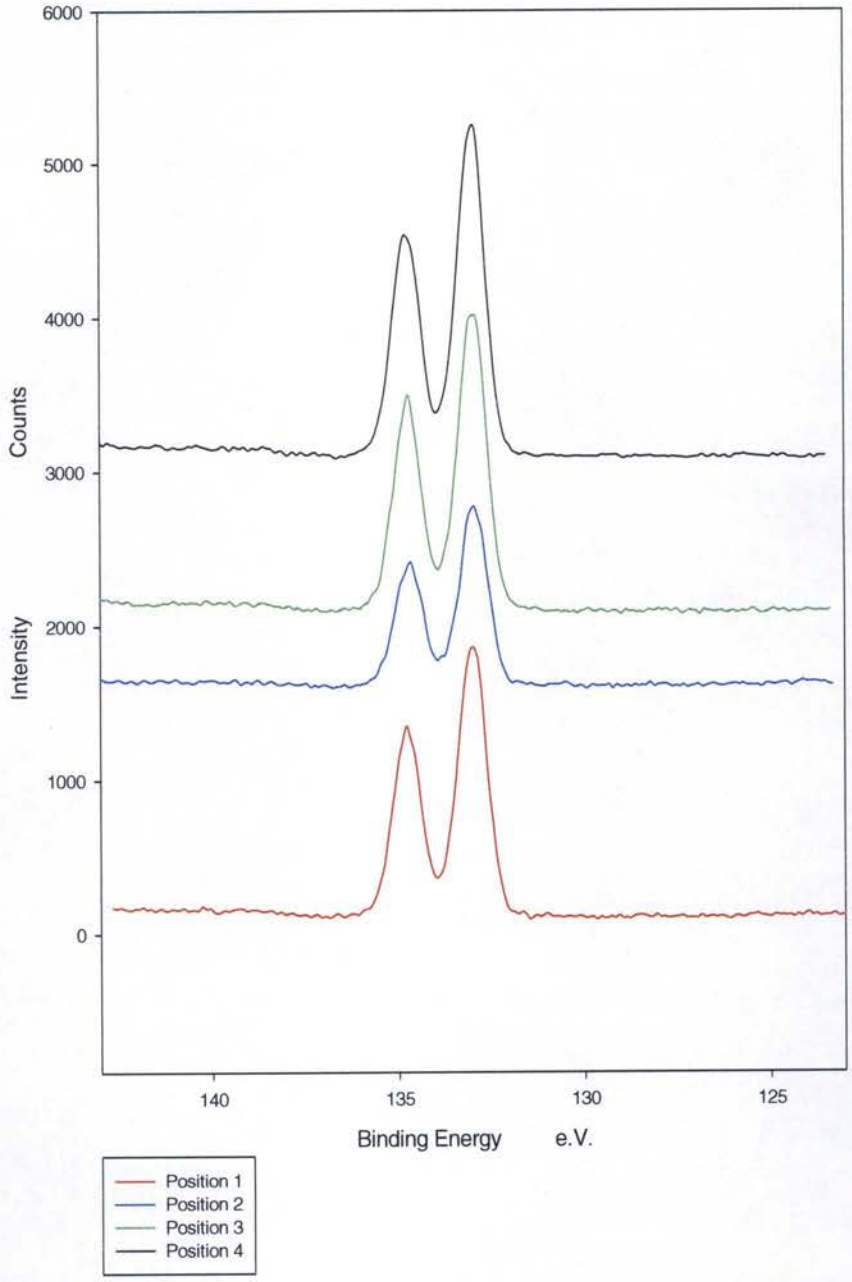

Figure 43: XPS spectra showing the Sr 3d peaks for a sample of strontium titanate exposed to 1.0 V for 20 hours. The positions start on the clipped end and begin to move away from it.

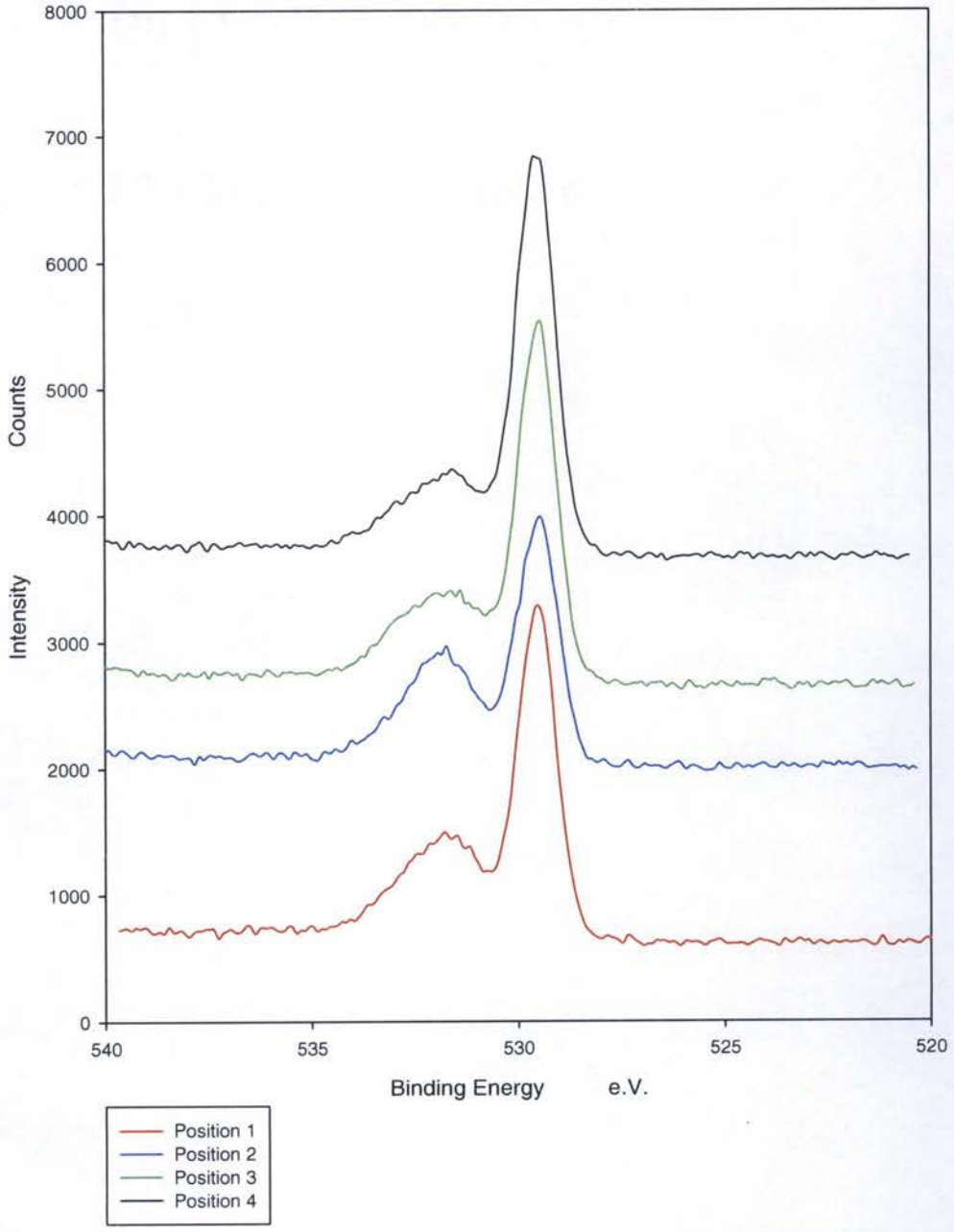

Figure 44: XPS spectra showing the O 1s peaks for a sample of strontium titanate exposed to 1.0 V for 20 hours. The positions start on the clipped end and begin to move away from it.

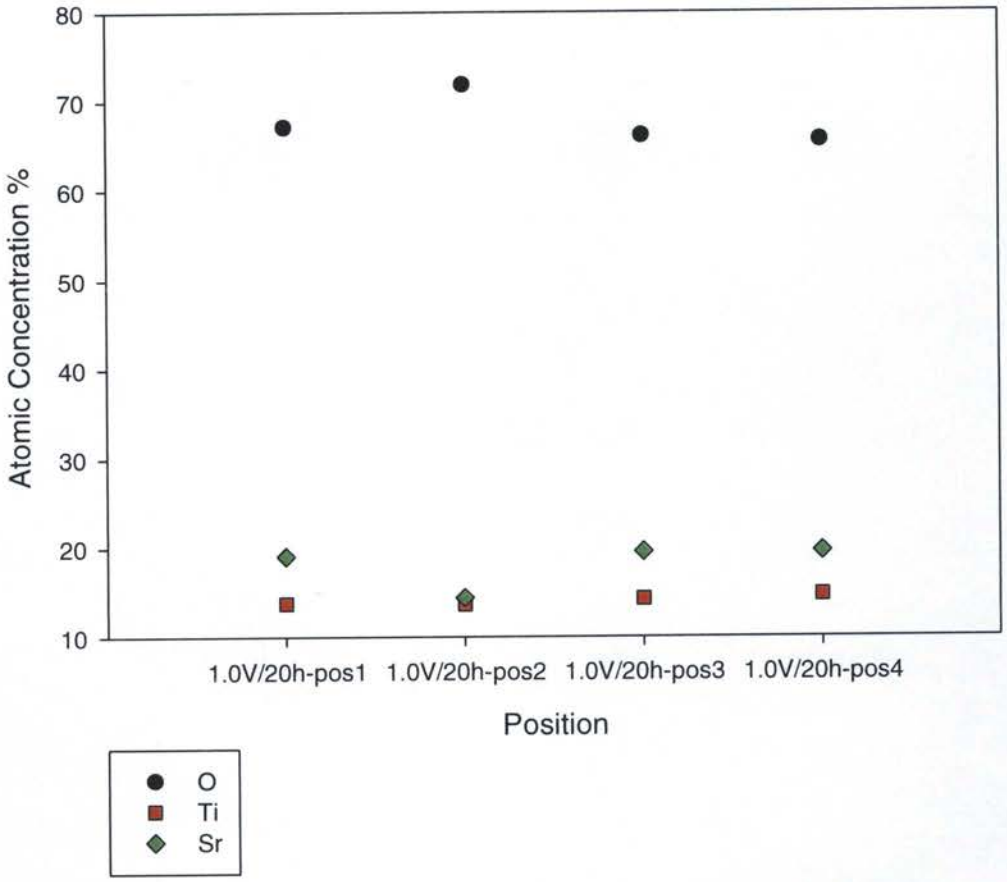

Figure 45: Quantitative analysis showing the atomic percentages of the various components for samples of strontium titanate exposed to 1.0 V for 20 hours. The positions start on the clipped end of the strontium titanate and move away from it.

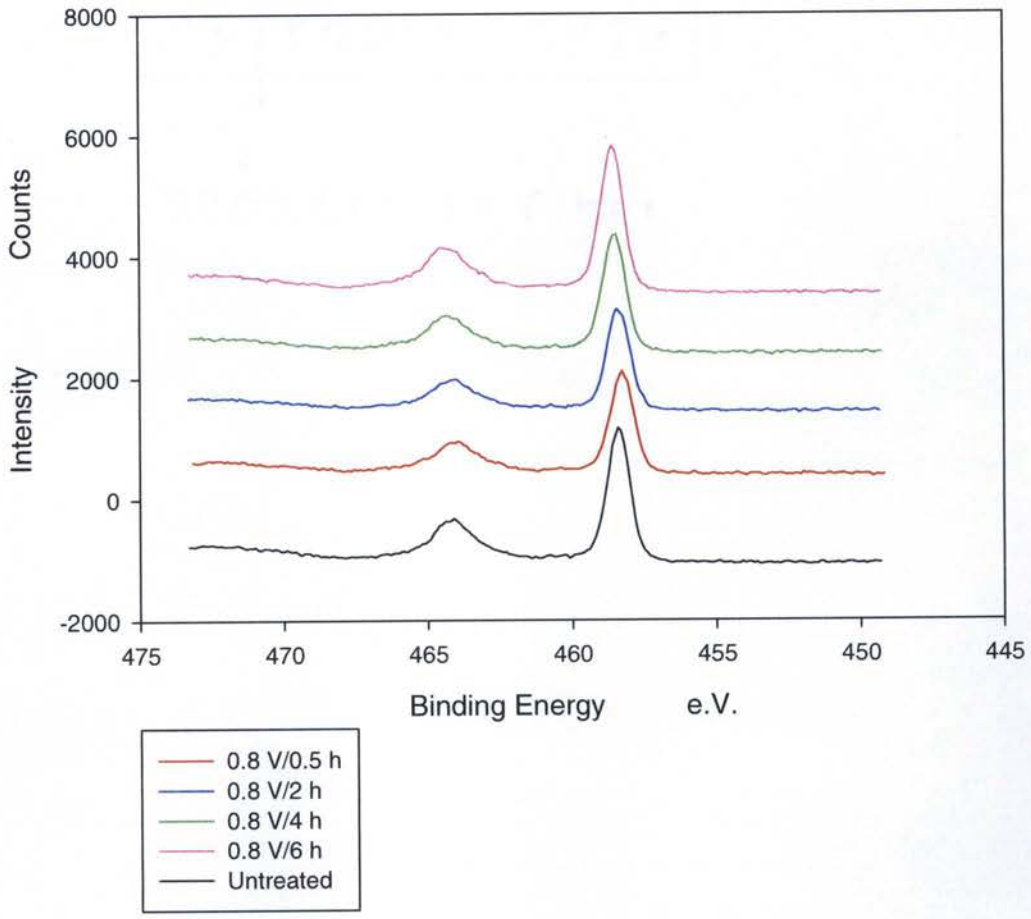

Figure 46: XPS spectra showing the Ti 2p peaks for samples of strontium titanate exposed to 0.8 V for various lengths of time. All data was taken from the clipped end.

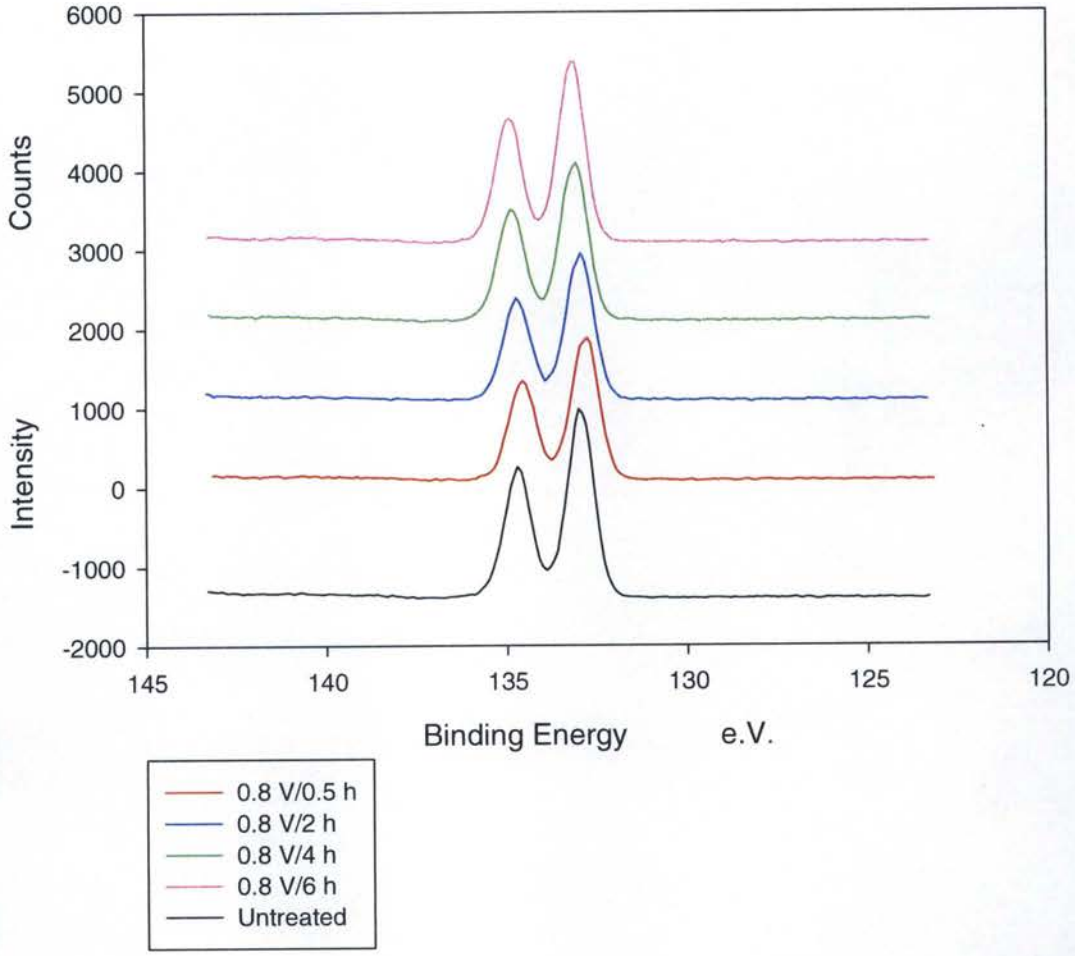

Figure 47: XPS spectra showing the Sr 3d peaks for samples of strontium titanate exposed to 0.8 V for various lengths of time. All data was taken from the clipped end.

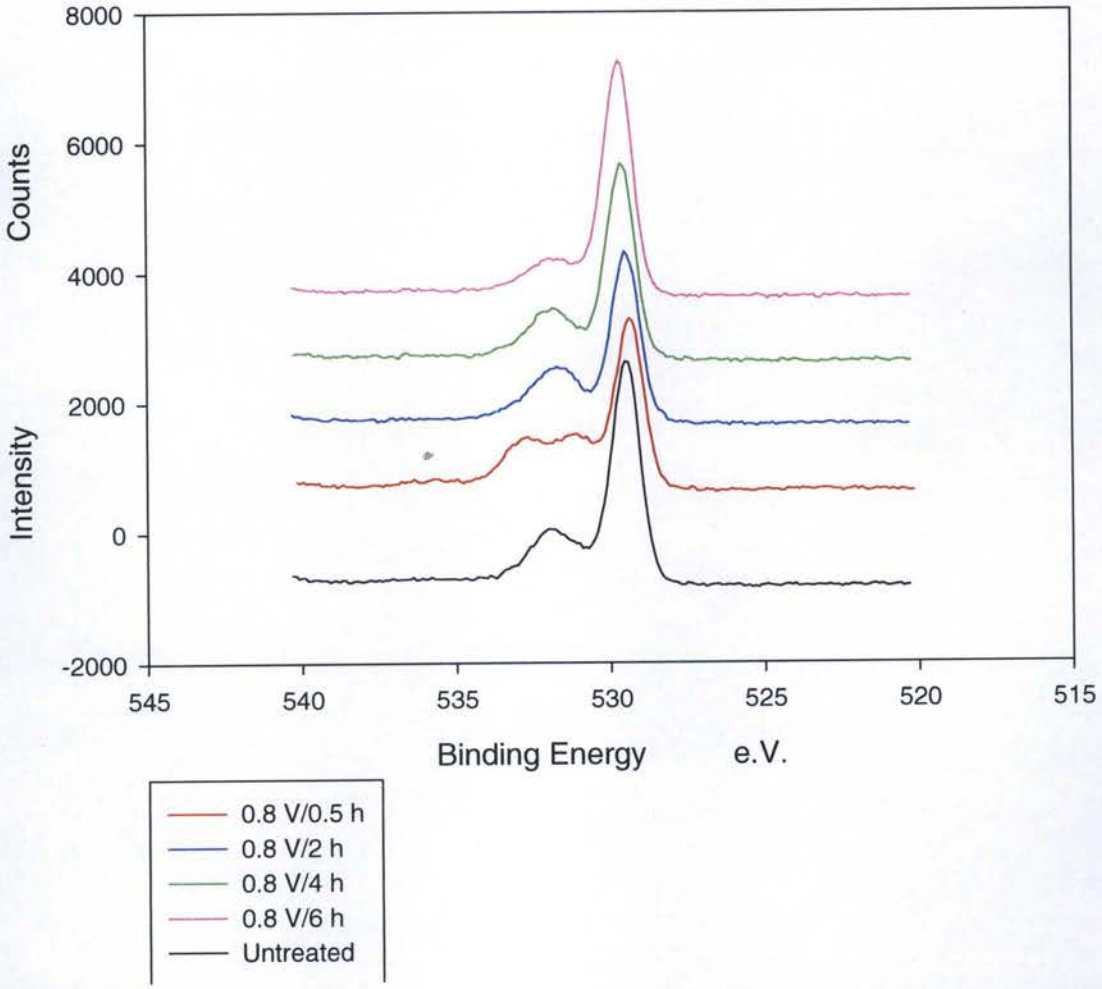

Figure 48: XPS spectra showing the O 1s peaks for samples of strontium titanate exposed to 0.8 V for various lengths of time. All data was taken from the clipped end.

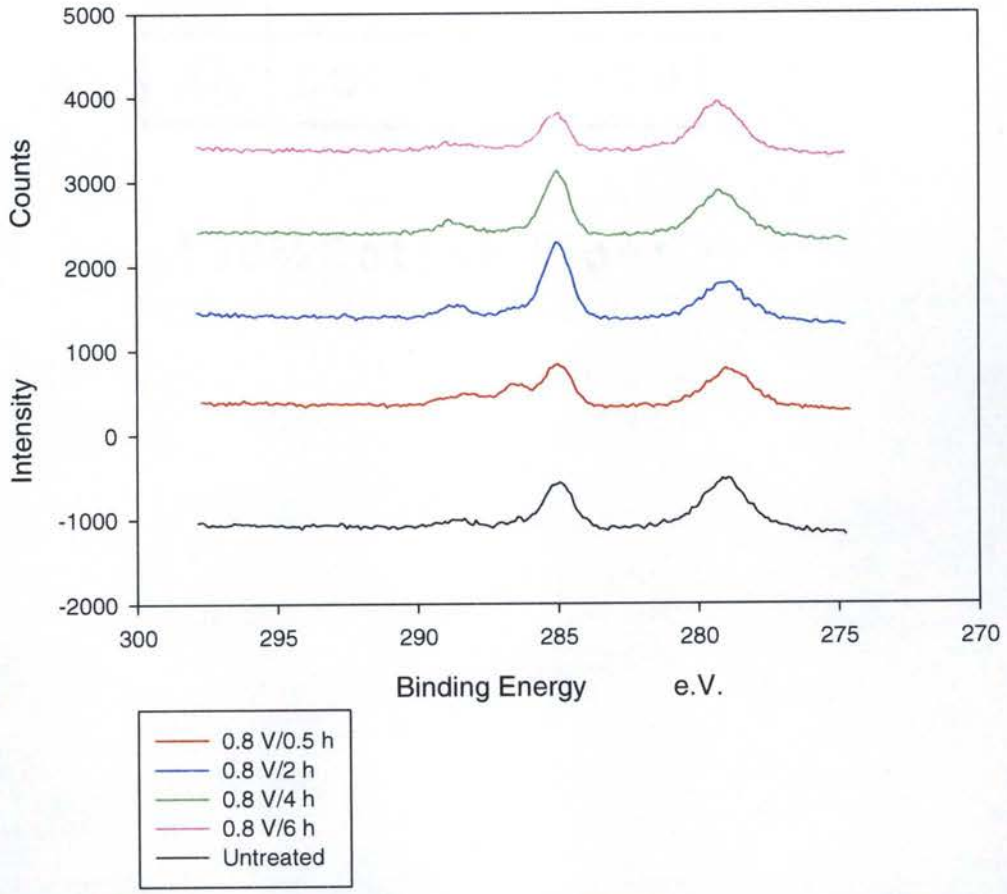

Figure 49: XPS spectra showing the C 1s peaks for samples of strontium titanate exposed to 0.8 V for various lengths of time. All data was taken from the clipped end.

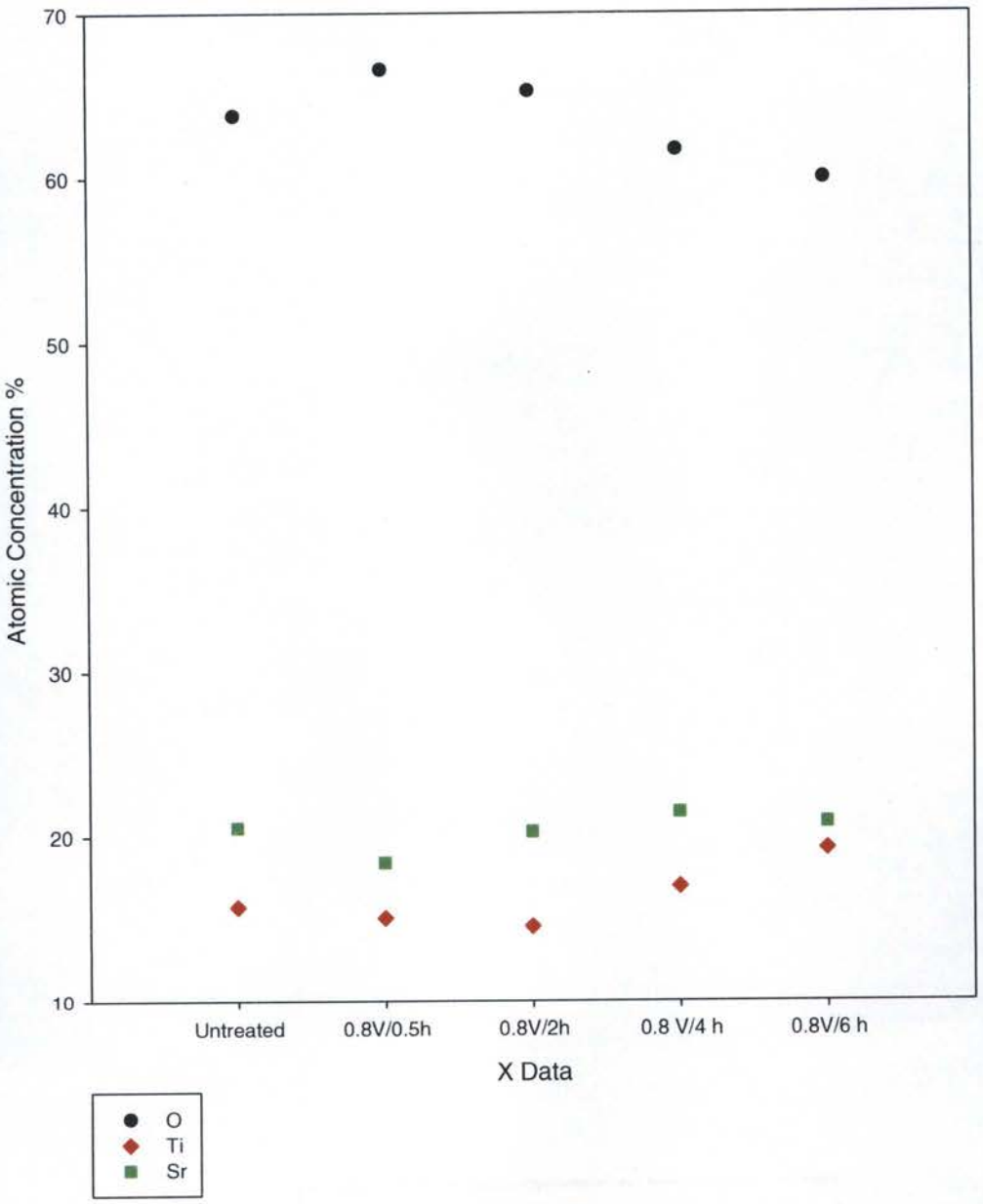

Figure 50: Quantitative analysis showing the atomic percentage of the various components for samples of strontium titanate exposed to 0.8 V for various lengths of time.

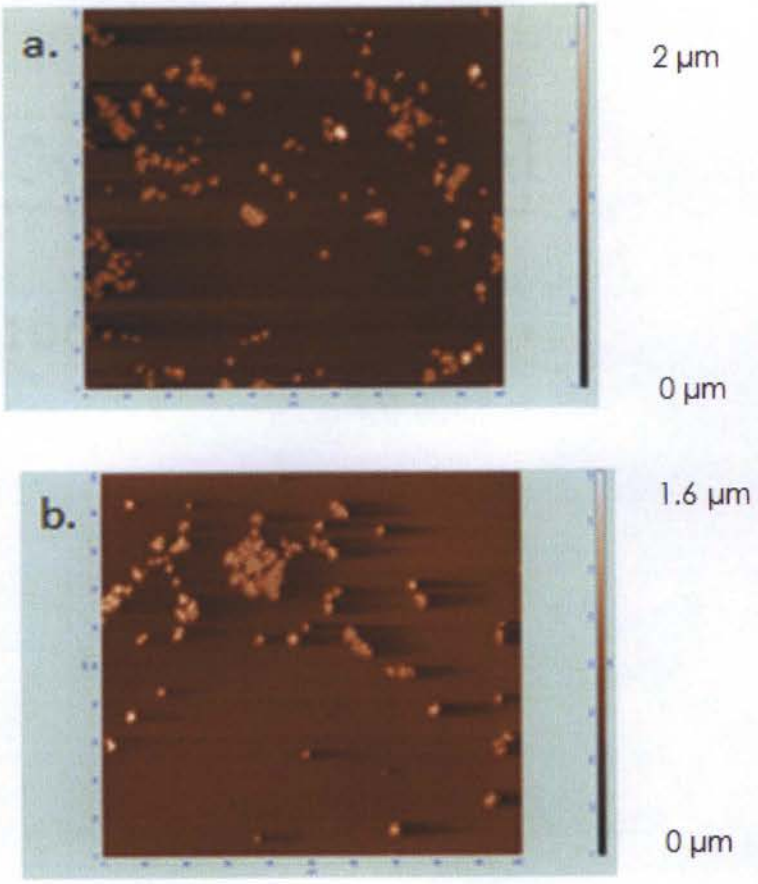

Figure 51: All micrographs are 100 µm x 100 µm and are taken from the clipped end of the same sample of strontium titanate. a.) After the initial exposure to 0.8 V for 20 hours. b.) After the follow-up exposure to -0.8 V for 20 hours.

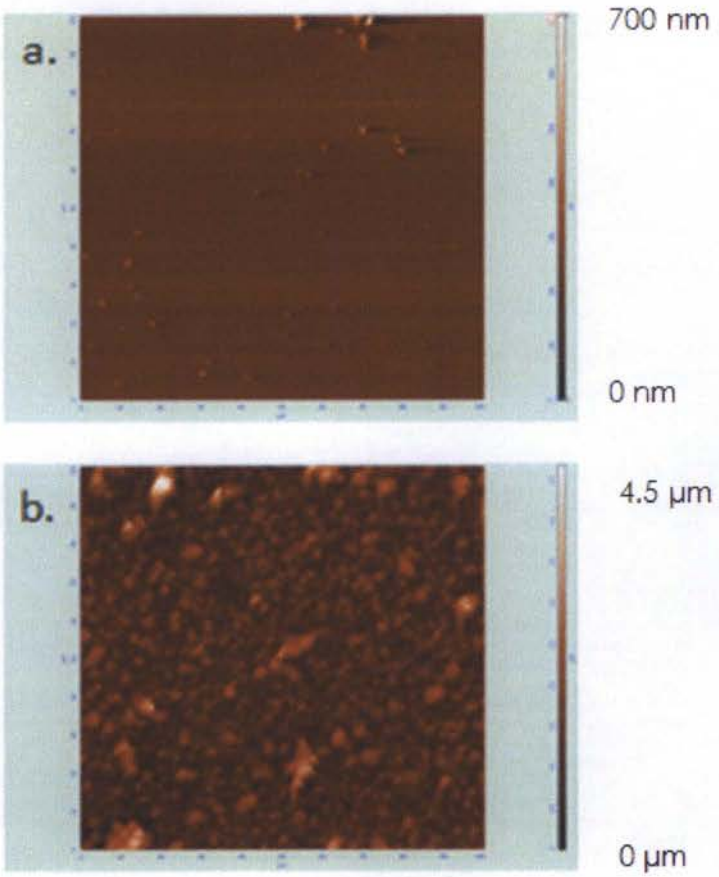

Figure 52: All micrographs are 100 µm x 100 µm; both are taken from the clipped ends of samples of strontium titanate exposed to 1.2 V for 20 hours. a.) With sonication in water. b.) Without sonication in water.

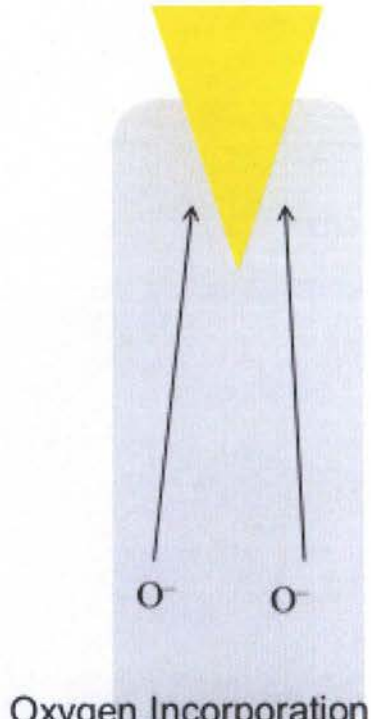

Oxygen Incorporation

$$A_xM_zO_y + 2\delta\ OH^- \leftrightarrow A_xM_zO_{y+\delta} + \delta\ H_2O + 2\ \delta\ e^-$$

Figure 53: Model for observed changes, oxygen species is absorbed into the strontium titanate and travels up the sample until it reaches the clipped area. Once there it can travel no further.

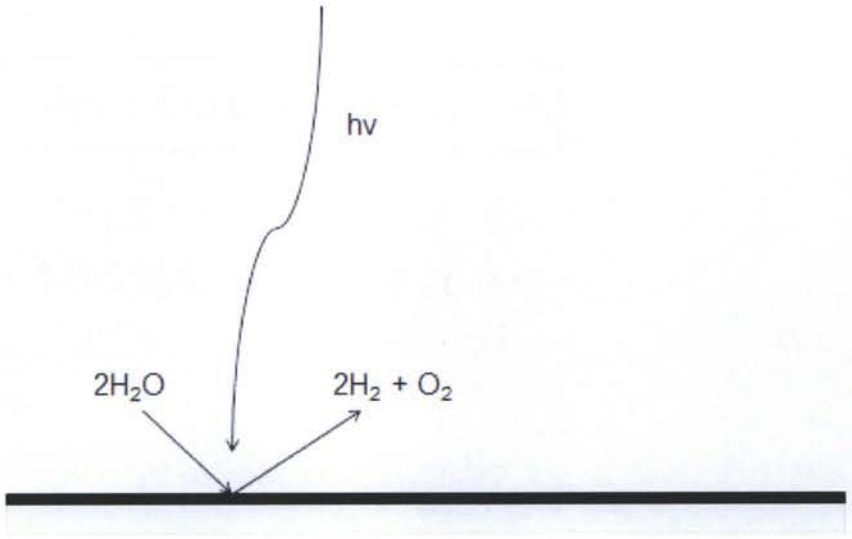

Figure 54: Illustration showing how container with titanium dioxide (in black) on strontium titanate substrate could be used as the photocatalyst for producing hydrogen gas from water.

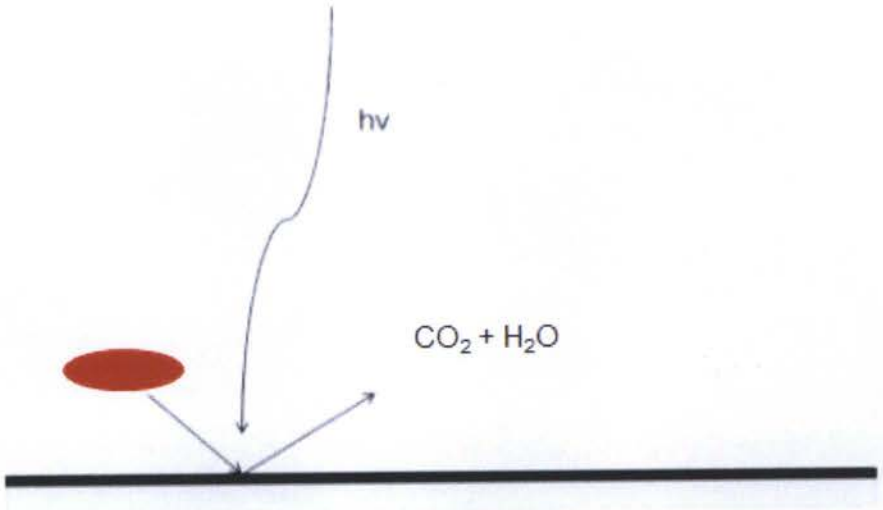

Figure 55: Illustration showing how container with titanium dioxide (in black) on strontium titanate substrate could be used as the photocatalyst for breaking down organic pollutants into water and carbon dioxide.